RESEARCH PROJECT COMPLETION REPORT

A LUMPED PARAMETER MODEL FOR THE EDWARDS AQUIFER

Project Number - SWTSU 92-1
September 1, 1992 - August 31, 1993
Grant Number
14-08-0001-G2048

by

Nisai Wanakule, Ph.D., P.E.
Roberto Anaya

The research on which this report is based was financed in part by the U. S. Department of Interior, Geological Survey, through the Texas Water Resources Institute. Non-Federal matching funds were provided by the Edwards Underground Water District, San Antonio, Texas, and Southwest Texas State University, San Marcos, Texas.

Contents of this publication do not necessarily reflect the views and policies of the Department of Interior, nor does mention of trade names or commercial products constitute their endorsement by the United States Government. Likewise, the contents of this publication have not necessarily been verified by and do not necessarily reflect the views of the Edwards Underground Water District and Southwest Texas State University.

All programs and information of the Texas Water Resources Institute are available to everyone without regard to race, ethnic origin, religion, sex, or age.

Technical Report No 163
Texas Water Resources Institute
The Texas A&M University System
College Station, TX 77843-2118

September 1993

TABLE OF CONTENTS

Table of Contents ii
List of Figures iv
ABSTRACT 1
Introduction 2
    Background Information 2
    Purpose and Scope of the Research 5
    Literature Review 5
Hydrogeology 6
Model Development 8
    Approach 10
    Lumped Parameter Model 12
    The Edwards Aquifer Conceptual Model 14
    Computer Model Algorithm 18
    Flow loss and Recharge Function 20
    Pumpage Estimation 25
Model Verification and Calibration 34
    Database Development 34
    Estimation of Parameters 34
    Optimization in Calibration Process 35
    Kalman Filtering 37
    Sensitivity Analysis 41
Summary and Conclusions 48
References 49
Appendix A: User's Manual 51
Appendix B: Computer Program Listing 56

A LUMPED PARAMETER MODEL FOR THE EDWARDS AQUIFER

ABSTRACT

A lumped parameter model has been developed to simulate monthly water levels and spring flows in the Edwards Aquifer. It is less complex and easier to use than the existing complex finite difference models for the Edwards Aquifer. The lumped parameter model was formulated using a discrete, nonlinear, nonstationary system based on control theory. The physical system of the Edwards Aquifer is conceptualized as a series of connected rock filled tanks representing major drainage basins of the aquifer. The model incorporates recharge functions derived from flow loss analysis of the drainage basins above and within the recharge area. The recharge functions estimate monthly recharge and allow for the interaction between groundwater and surface water for each drainage basin. Pumpage distribution coefficients were derived for each drainage basin to estimate monthly pumpage values. Monthly stream gage and aquifer water level data were used for calibrating and verifying the model. Model parameters were obtained with the aid of a nonlinear optimization algorithim. A Kalman filter was used to improve simulation results. The lumped parameter model proved to be very efficient in simulating 189 monthly iterations of water levels for nine drainage basins in less than four minutes on a 68040 based microcomputer. The model should prove useful for assessing pumpage regulations necessary to maintain springflows under historic drought conditions and for exploring management alternatives for the Edwards Aquifer. Future plans and research consist of re-coding the model as a spreadsheet function and perhaps using a Laplace transform as a solution method. Other research should include generalizing the model for use in other karst aquifers, integrating the model with a rainfall-runoff model, and developing a better method for estimating recharge.

INTRODUCTION

The entire Edwards (Balcones Fault Zone) Aquifer extends along the narrow belt of the Balcones Fault Zone from north of Georgetown through Austin, San Marcos, New Braunfels, San Antonio, Hondo, Sabinal and Uvalde to Brackettville. This limestone aquifer is separated into three portions by groundwater divides at Kyle in Hays county and at the Colorado River. The central portion, from Kyle to Colorado River is referred to as the Barton Springs segment. The part between the Colorado River and Salado, in Bell County is referred to as the northern segment of the Edwards Aquifer. This study will focus on the western portion, referred to as the San Antonio region. The Edwards Aquifer to be referred to hereafter will be restricted to the San Antonio region.

The Edwards Aquifer is approximately 160 miles in length from Brackettville to Kyle and varies in width from 5 to 40 miles. It extends to cover the major part of five counties namely, Uvalde, Medina, Bexar, Comal and Hays (see Figure 1). It traverses several streams in three major river basins including the Nueces, San Antonio and Guadalupe. The aquifer is a very unique carbonate aquifer located in south-central Texas. Karst characteristics of the Edwards Aquifer make it one of the most productive aquifers in the United States and yet groundwater flow within the aquifer is very complex and difficult to predict. The Edwards Aquifer is designated by the EPA as a "sole source" drinking water supply for the 1.5 million people of San Antonio and the Austin-San Antonio corridor. The aquifer is also vital to the agricultural and light industrial economy of the region. Springflows from the Comal and San Marcos Springs provide water for the tourist and recreation industry, critical habitat of several endangered species, appropriated water use downstream on the Gulf Coastal Plain, and the San Antonio Bay ecosystem.

Background Information

Early Europeans first settled along perennial streams sustained by natural spring flows from the Edwards Aquifer (Maclay and Land, 1988). Substantial well discharge from the aquifer began in the late 1800's and steadily increased from 101,900 ac-ft in 1934 to a record high of 542,400 ac-ft in 1989. The groundwater is used extensively for public water supply and agriculture, and accounted for, respectively, 56.6% and 30.1% of the total well discharge during 1981-90. The continual increase in well discharge has had an effect on the natural spring

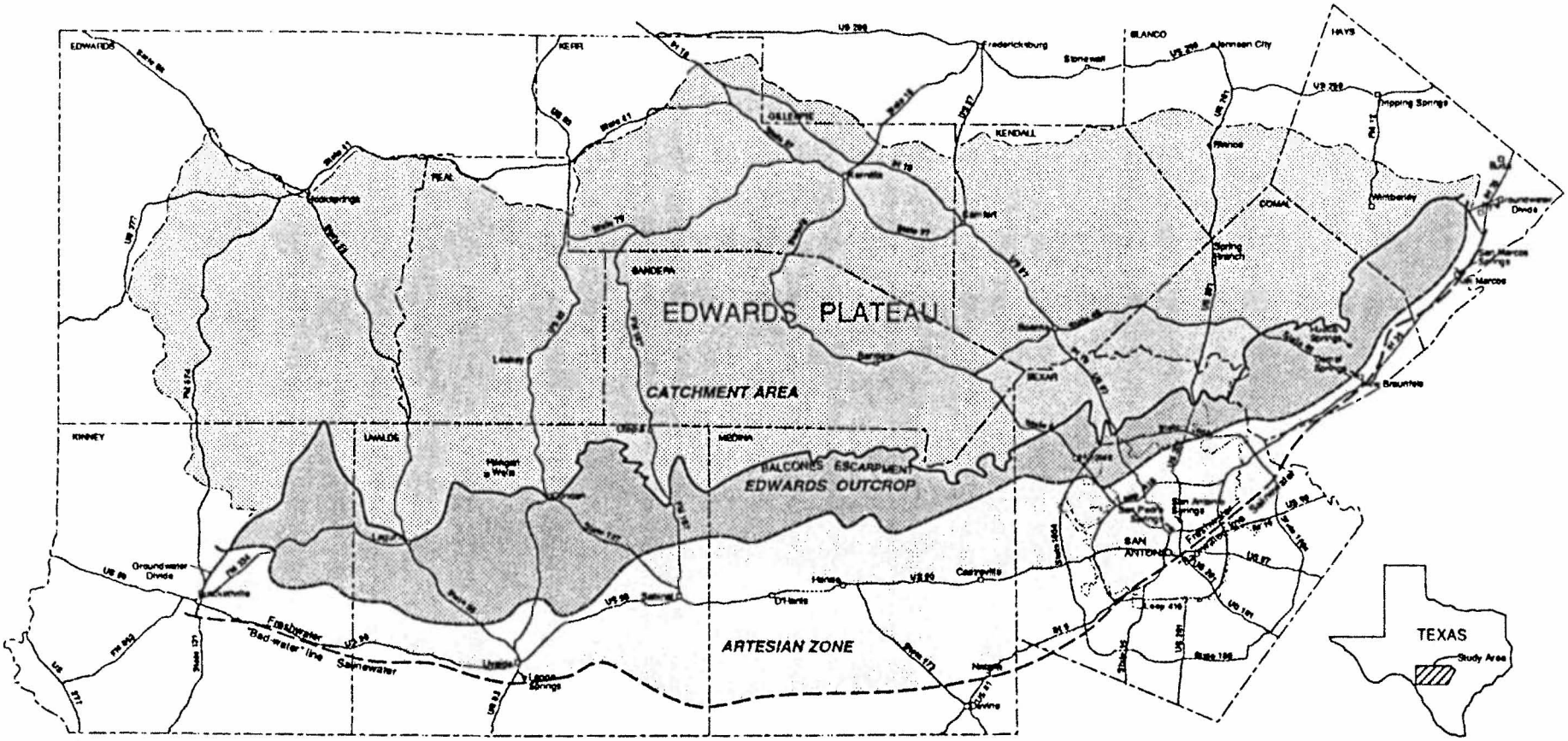

Figure 1. Physiographic location of the Edwards Aquifer (San Antonio Region)

discharge, which comprises 42.2% (1981-90) of the total withdrawal from the Edwards Aquifer. San Pedro and San Antonio Springs in San Antonio have become intermittent. Historically, the Comal Springs stopped flowing for two months in the summer of 1956. In 1984 and 1990, some of the higher Comal Springs ceased to flow and water levels in the index well (J17) dropped to within twelve feet of the 1956 record low.

Major problems facing the Edwards Aquifer are the threat of overdrafting the average annual recharge and maintaining natural springflows. Accordingly, the Edwards Underground Water District (EUWD) was authorized by the state legislature to develop, implement, and enforce a Drought Management Plan (DMP). The Cities of San Antonio, New Braunfels, and San Marcos have had to enforce Water Conservation Plan ordinances and water use disputes among aquifer users have become more frequent. In the most current case, the Sierra Club sued the Secretary of the Interior and the U.S. Fish and Wildlife Service (FWS) for failure to perform duties under the Endangered Species Act (ESA) and for injunctive relief. The U. S. District Court for the Western District of Texas reached a decision on January 30, 1993, and ordered FWS to determine required springflows, and the Texas Water Commission (TWC, now the Texas Natural Resource Conservation Commision or TNRCC) to prepare a plan assuring that springflows will not drop below jeopardy levels. The court threatened additional orders if the state legislature did not set up a regulatory system to limit withdrawals from the aquifer. In response, the 73rd Texas Legislature passed the Senate Bill No. 1477 to create the Edwards Aquifer Authority (EAA) and abolish the EUWD, effective September 1, 1993. Governed by an appointed Board of Directors, the authority's primary function is to regulate the aquifer pumpage by limiting the long-term annual withdrawal to 400,000 ac-ft. This amount is believed to be adequate to maintain the flows at the Comal and the San Marcos Springs, although the court opinion stated this level to be 200,000 ac-ft. Aquifer modeling is a part of the effort to improve the understanding of quantitative relationships among recharge, pumpage, spring-flow, and water levels. Such models will allow efficient and prudent management options to be explored without actually implementing a plan that would cause jeopardy to or loss of federally-listed endangered species.

Purpose and Scope of the Research

For the Edwards Aquifer to be successfully managed, an accurate, near real-time simulation model is needed in addition to institutional changes and new legislation. Existing models are too complicated and difficult to use in real-time management practices for pumpage control. The use of distributed parameter models such as a finite difference model require massive data input, calculate unwarranted intermediate steps, and generate a bulk of unnecessary output, and yet have not yielded satisfactorily accurate simulations.

The purpose of this research is to develop and test a lumped parameter model for simulating monthly water levels and springflows of the Edwards Aquifer. The goal of the new model is to keep it simple and easy to use without sacrificing simulation accuracy and to allow for advanced research using stochastic optimization in groundwater management. In addition, this study performs flow loss analysis to determine recharge functions for each river basin. These functions will provide a mechanism for the groundwater model to interact with surface runoff which has not been considered in previous models. Instead of taking recharge as a fixed input, the model will calculate recharge using streamflow input and allows recharge to vary with aquifer water levels.

The scope of the research is limited to the Edwards Aquifer, Balcones Fault Zone of the San Antonio Region. The data used for calibrating and verifying the model will consist of stream and spring flow data from the United States Geological Survey (USGS), well data from the Texas Natural Resources Information Systems (TNRIS), Texas Water Development Board (TWDB) and the Texas Water Commission (TWC).

Literature Review

Most of the conventional aquifer simulation models, such as PLASM (Prickett and Lonnquist, 1971), USGS-2D-FLOW (Trescott et al., 1976), and MODFLOW (McDonald and Harbaugh, 1988), were developed based on a distributed parameter finite-difference model. A list of other distributed parameter models using finite elements can also be found in van der Heijde et al. (1988). These distributed parameter models were developed based on the alluvial type aquifers, in which groundwater moves slowly through the small pores of a porous matrix. In contrast, groundwater in a karst aquifer, having the characteristics of channelization and

large cavities, flows rapidly through conduit networks similar to a water distribution system. Previous karst aquifer modeling has been done with the above mentioned finite-difference models. For example, Klemt, et al. (1978) and Maclay and Land (1988) modified PLASM and USGS-2D-FLOW, respectively, to develop planning models for the Edwards Aquifer. Despite using an annual time-step, they still required massive data input since the model contained over 800 active cells. Thorkildsen and McElhaney (1992) refined and calibrated the former model for use in evaluating management scenarios. The model had monthly time-steps and encountered some difficulties in calibration and verification.

The source of recharge to the Edwards Aquifer is from stream flow loss and infiltration due to precipitation over the Edwards outcrop area. Methods of estimating natural recharge to the Edwards Aquifer were developed by the USGS (Garza, 1966; Puente, 1978) and HDR Engineering, Inc. (Choffel and Vaugh, 1993). Although both methods produced similar annual historic recharge estimates, they differed in spatial and temporal distributions. The principal difference in the two methods was in calculating runoff in the drainage area between the upper and lower stream gages. The USGS method assumed that precipitation-runoff conditions were the same for the catchment and recharge areas and calculated runoff from the intervening area based on the per-unit-area streamflow at the upper gage. When precipitation within the catchment and recharge areas differ by more than 20 percent, linear adjustments were made according to a precipitation ratio. Adjustments were also made for baseflows within each basin using baseflow recession curves developed by Puente (1975).

HDR calculated runoff in the intervening drainage area with a modified version of the Soil Conservation Service (SCS) runoff curve number method. The method accounted for spatial variation in precipitation by using the Thiessen Polygon procedure. Soil cover differences and water rights diversions were also accounted for in the HDR method. The HDR method indicated a greater contribution to total estimated recharge from the Guadalupe River Basin and less from the Nueces River Basin than that calculated by the USGS.

HYDROGEOLOGY

Table 1 shows the stratigraphic units of a typical Edwards Aquifer cross section. The aquifer is an association of Lower Cretaceous limestones overlying the Glen Rose Limestone and underlying the Del Rio Clay. The base of the aquifer is

Table 1. Stratigraphic units of the Edwards Aquifer

AGE		MAVERICK BASIN	DEVILS RIVER TREND	SAN MARCOS PLATFORM	HYDRO-GEOLOGY
CRETACEOUS	UPPER	DEL RIO CLAY	DEL RIO CLAY	DEL RIO CLAY	CONFINING UNIT
	LOWER	SALMON PEAK FORMATION	DEVILS RIVER LIMESTONE	GEORGETOWN FORMATION	EDWARDS AQUIFER
		McKNIGHT FORMATION		PERSON FORMATION	
		WEST NUECES FORMATION		KAINER FORMATION	
		GLEN ROSE FORMATION	GLEN ROSE FORMATION	GLEN ROSE FORMATION	CONFINING UNIT

Modified from Maclay and Land, 1988

confined by the upper part of the Glen Rose Formation and in the artesian section, the top of the aquifer is confined by the Del Rio Formation. The lateral boundaries of the Edwards Aquifer consist of groundwater divides on the east and west near Kyle in Hays County and near Brackettville in Kinney County, respectively. The aquifer is bounded on the south by the "bad water line", (line marking water with more than 1000 mg/l of total dissolved solids), and on the north by the northern most edge of the Balcones Fault Zone.

The Edwards Group and associated limestones were deposited as shallow marine platform carbonates consisting of reef and deep marine lithofacies in the western portion of the aquifer region. Most of the Edwards Group and associated limestones within the San Marcos Platform and the Devils River Reef Trend were

subjected to subaerial exposure after deposition which enhanced the development of secondary porosity (Maclay and Land, 1988). Enhanced porosity has also occurred along the high angle faults and fractures of the Balcones Fault Zone.

The Edwards Aquifer receives water primarily from streams and rivers originating from the catchment areas on the Edwards Plateau (Figure 2). Streams and rivers that cross the outcrop of the Edwards Aquifer lose major portions of their flow to the aquifer through joints, faults, and sink holes. There are three river basins that cross the aquifer area: the Nueces, the San Antonio, and the Guadalupe River. Extending from the west, the Nueces River Basin covers over a half of the aquifer area. Several major tributaries in the basin traverse the aquifer recharge zone including the Nueces; the West Nueces; the Frio; the Dry Frio; and the Sabinal Rivers; as well as the Seco and the Hondo Creeks. The portion of the San Antonio River Basin that is located in the recharge zone extends from the Medina River to the Cibolo Creek and includes headwaters of the Helotes, Leon, and Salado Creeks. Only a small portion of the Guadalupe River Basin intersects the eastern aquifer area. However, two of the basin tributaries, the Comal and San Marcos Rivers, are primarily fed by the aquifer at the Comal and San Marcos Springs. The tributaries crossing the recharge area include the Guadalupe River, the Blanco River, and tributary headwaters of the Comal and San Marcos Rivers. Small creeks in the headwaters are the Dry Comal, Alligator, York, Purgatory, and Sink Creeks.

Based on the USGS estimates, the aquifer has an average annual recharge of 651,700 ac-ft with about 58.5% contributed by the Nueces River Basin. Generally, the water flows south-southeastward from the recharge zone under steep hydraulic gradients and low permeabilities within the unconfined portion of the aquifer. As the water flows into the confined portion of the aquifer, the flow direction changes toward the east and northeast within the low gradient, highly permeable grabens in the artesian zone. The water then discharges from several springs — mostly the Comal and San Marcos Springs — which account for 355,500 ac-ft annually. The two major springs contribute about 25% of the flow in the Guadalupe River downstream. The contribution was about 66% during the drought year of 1956.

MODEL DEVELOPMENT

A first step in the modeling process involves selecting the type of system to be represented. A *lumped parameter* model considers mixed effects of the system

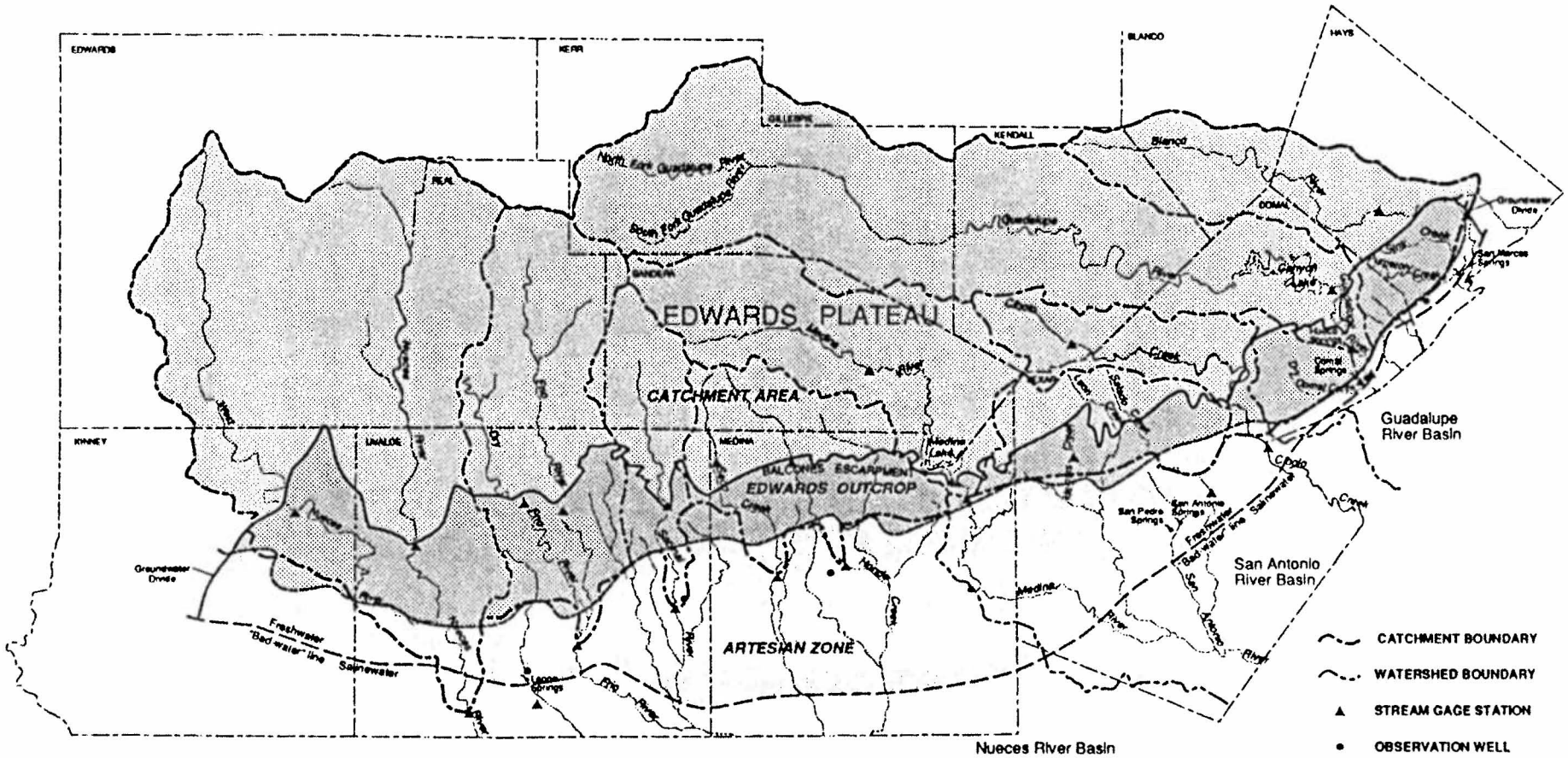

Figure 2. Streams and river basins that cross the Edwards Aquifer recharge zone

composed of ideal elements having uniform characteristics. In contrast, a model represented by a heterogeneous system consisting of infinitely small elements is called a *distributed parameter* model. Thus, it is expressed by partial rather than ordinary differential equations. A system is said to be *linear* if the system output can be produced by superposition. Furthermore, a system whose parameters change with time is called *nonstationary*, otherwise it is called *stationary*.

The following sections will discuss in some detail the development of a lumped parameter model for the Edwards Aquifer. The model is formulated based on the state-space point of view in control system theory (Takahashi, et al., 1972). A discrete, nonlinear, nonstationary system is used to conceptualize the physical system of the Edwards Aquifer, which consists of a series of connected leaking tanks. The model is focused on simulating monthly water levels at key observation wells in eight river sub-basins and two springflows at Comal and San Marcos. Built-in recharge functions for each sub-basin are also developed to estimate monthly recharge from streamflow input. They allow for the interaction between ground-water and surface water to occur.

First, the basic differential equations and their solutions will be presented. Then, the tank model and the Edwards conceptual model will be discussed. Finally, the solution algorithm and computer program will also be described.

Approach

Differential equations for lumped parameter models and their solutions are presented below. Their derivations can be found in Takahashi, et al. (1972).

The first order ordinary differential equation (ODE) for a linear stationary system can be represented as:

$$\frac{d}{dt}x(t) = Ax(t) + Bu(t) \tag{1}$$

where u is the control input, x is the system state, and A and B are system parameters. The solution of the above equation for a general u(t) is

$$x(t) = e^{At}x_0 + \int_0^t e^{A(t-\tau)}Bu(\tau)d\tau , \tag{2}$$

where x_0 is the initial value of x(t), and τ is a dummy variable of integration. The first term of the solution (2) is called the *free response* as opposed to the *forced*

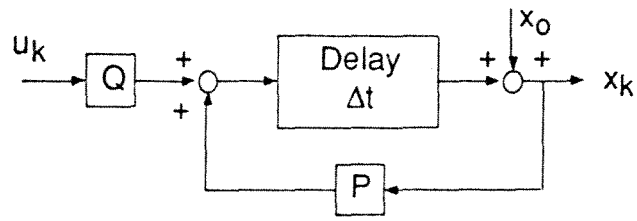

Figure 3. Graphical representation of a first-order, linear, stationary system

response for the second term. For a discrete system with Δt time interval, one can apply the above solution for a period from $k\Delta t$ to $(k+1)\Delta t$ and solve

$$x_{k+1} = x[(k+1)\Delta t] = e^{A\Delta t} x_k + \int_{k\Delta t}^{(k+1)\Delta t} e^{A[(k+1)\Delta t-\tau]} Bu_k d\tau$$

$$= e^{A\Delta t} x_k + (e^{A\Delta t} - 1) A^{-1}Bu_k$$

$$= Px_k + Qu_k , \tag{3}$$

where $P = e^{A\Delta t}$ and $Q = (P-1)A^{-1}B$. The computational scheme following the above equation is graphically shown in Figure 3. The response x_k at time $t = k\Delta t$ can be computed by repeatedly applying of equation (3) resulting in

$$x_k = P^k x_o + \sum_{i=0}^{k-1} P^{k-1-i} Qu_i \tag{4}$$

For a higher order system, the solution can be generalized with the aid of vector calculus. Considering an nth order system of n state variables $(x_1,x_2,\ldots,x_n)$ with r inputs $(u_1,u_2,\ldots,u_r)$, the scalar equation (1) becomes a vector differential equation

$$\frac{d}{dt}\mathbf{x}(t) = \mathbf{A}\mathbf{x}(t) + \mathbf{B}\mathbf{u}(t) \tag{5}$$

where **x** and **u** are vectors of state and input variables, respectively. **A** and **B** are constant parameter matrices with dimensions of $n \times n$ and $n \times r$, respectively. The matrix difference equation equivalent to (3) can be expressed as

$$\mathbf{x}_{k+1} = e^{\mathbf{A}\Delta t}\,\mathbf{x}_k + e^{\mathbf{A}\Delta t}\int_0^{\Delta t} e^{-\mathbf{A}\tau}\,\mathbf{B}\mathbf{u}(\tau)d\tau$$

$$= e^{\mathbf{A}\Delta t}\,\mathbf{x}_k + e^{\mathbf{A}\Delta t}(\mathbf{I} - e^{-\mathbf{A}\Delta t})\,\mathbf{A}^{-1}\mathbf{B}\mathbf{u}_k$$

$$= e^{\mathbf{A}\Delta t}\,\mathbf{x}_k + (e^{\mathbf{A}\Delta t} - \mathbf{I})\,\mathbf{A}^{-1}\mathbf{B}\mathbf{u}_k$$

$$= \mathbf{P}\mathbf{x}_k + \mathbf{Q}\mathbf{u}_k\,, \tag{6}$$

where,

$$\mathbf{P} = e^{\mathbf{A}\Delta t}\,, \qquad \mathbf{Q} = (\mathbf{P} - \mathbf{I})\mathbf{A}^{-1}\mathbf{B}\,, \tag{7}$$

The exponential matrix $e^{\mathbf{A}\Delta t}$ is also called the state-transition matrix and has an $n \times n$ dimension for an $n \times n$ matrix $\mathbf{A}$. The matrix can be evaluated using the following series expansion,

$$e^{\mathbf{A}\Delta t} = \mathbf{I} + \mathbf{A}\Delta t + \frac{1}{2!}\mathbf{A}^2(\Delta t)^2 + \frac{1}{3!}\mathbf{A}^3(\Delta t)^3 + \ldots \tag{8}$$

Equation (6) is applied repeatedly starting from $\mathbf{x}_0$ and the result can be written similar to (4)

$$\mathbf{x}_k = \mathbf{P}^k\mathbf{x}_0 + \sum_{i=0}^{k-1} \mathbf{P}^{k-1-i}\,\mathbf{Q}\mathbf{u}_i \tag{9}$$

Lumped Parameter Model

Attention is turned to the derivation of the governing differential equation by the aid of a conceptual tank model. The modeling concept is similar to the hydrologic routings of river, watershed, and reservoir hydrographs used by surface water hydrologists. The lumped parameter conceptual model of the surface and ground water flow in the area below the upper gages of the Nueces River Sub-Basin is shown in Figure 4. The source or sink $u_1(t)$, is the combined flow of the upper gages less pumpage and flow at the lower gage of a rock-filled tank with storage and transmissivity related parameters S_1 and T_1, respectively. The output $y_1(t)$ is the underflow to the nearby system, the Frio River Sub-Basin. The state variable $x_1(t)$ is the flow-driven potential, which can be expressed as the water level in an

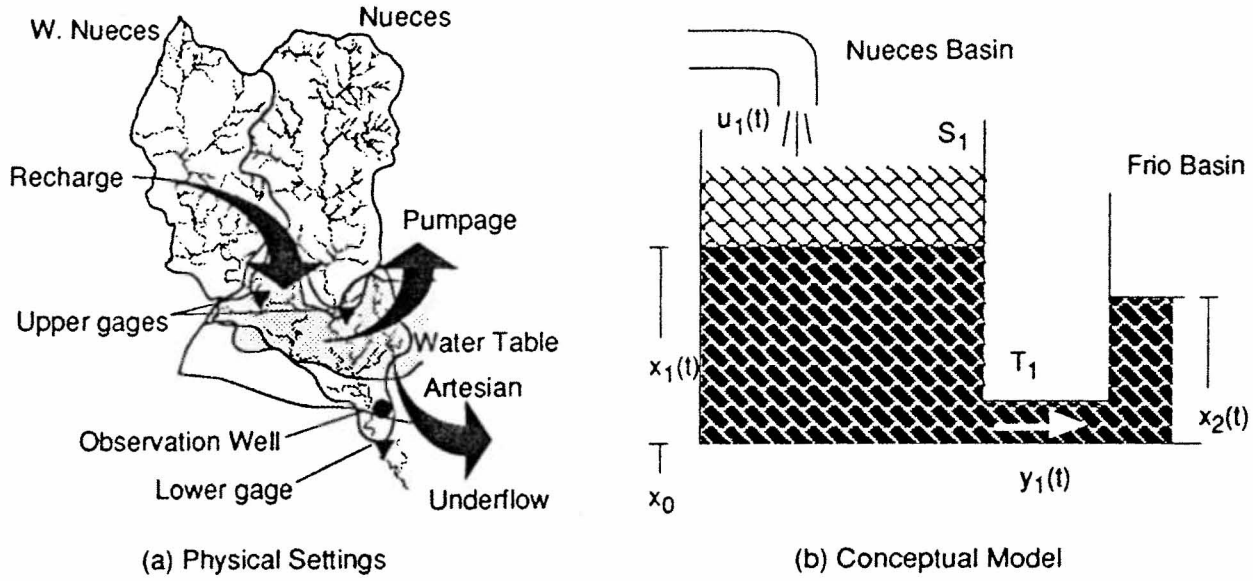

Figure 4. Recharge and water level relationships for the Edwards Aquifer in the Nueces River Basin and underflow to the Frio River Basin

observation well near the lower gage. S_1 and T_1 are conceived as aggregate or lumped parameters for surface and groundwater flow in the intermediate area between the upper and the lower gages. Using the lumped parameter concept, the aquifer portion under the Nueces can be considered as an elementary control volume of water in a homogeneous medium as opposed to multiple cells in a finite difference distributed parameter model. The flow regime becomes isotropic and can be described by a single continuity, or mass balance equation. The resulting system differential equation describing groundwater flow under the Nueces River Sub-Basin can be derived as follows:

$$u_1(t) - y_1(t) = \frac{d\forall}{dt}, \tag{10}$$

where $\forall$ is the volume of water under the sub-basin and can be expressed as a function of x_1:

$$\forall(x_1) = S_1'(x_1 - x_0)^n, \tag{11}$$

where S_1' is the storage constant related to aquifer porosity, the exponent n is related to the volumetric geometry, and x_0 is the aquifer base elevation for the sub-basin. Equation (11) can then be expressed as:

$$\frac{d\forall}{dt} = S_1' n(x_1-x_0)^{n-1}\frac{dx_1}{dt} = S_1(x_1)\frac{dx_1}{dt}, \tag{12}$$

where the storage related parameter $S_1(x_1) = S_1' n(x_1-x_0)^{n-1}$. For a linear storage model, i.e. n = 1 in equation (11), S_1 becomes a constant and is equal to S_1'.

Applying Darcy's Law, the underflow, $y_1(t)$ may be expressed as:

$$y_1(t) = K\frac{(x_1-x_2)}{L}A, \tag{13}$$

where; K is the hydraulic conductivity, $(x_1-x_2)/L$ is the hydraulic gradient, A is the cross-sectional area of the flow path, L is the representative distance of the flow path, and x_2 is the potential in the adjacent sub-basin, (the Frio River Basin). If w is the average cross-sectional width along the flow path, then by substitution, equation (13) becomes:

$$y_1(t) = K\frac{(x_1-x_2)}{L}(x_1-x_0)w = T_1'\frac{(x_1-x_2)}{L}w = T_1(x_1-x_2), \tag{14}$$

where $T_1'(x_1) = K(x_1-x_0)$ is the transmissivity, (x_1-x_0) is the average aquifer thickness, and $T_1 = T_1'w/L$ is the aggregate transmissivity related parameter which depends on a flow path geometry. For an artesian condition, the aquifer thickness becomes a constant independent of x_1 and so does T_1'. By substituting equations (12) and (14) back into equation (10), the mass balance equation can be expressed as:

$$u_1(t)-T_1(x_1-x_2) = S_1(x_1)\frac{dx_1}{dt}, \tag{15}$$

which can be rearranged to the canonical form (1) as:

$$\frac{dx_1}{dt} = \frac{T_1}{S_1}x_1(t) + \frac{1}{S_1}u_1(t) \tag{16}$$

The Edwards Aquifer Conceptual Model

Watersheds of the streams that cross the aquifer recharge zone can be divided into nine sub-basins. Although, The Edwards Underground Water District (Wokhour,1993) suggests that the Guadalupe River Basin may recharge the aquifer during low water levels, data was not available to us during our research to confirm this recharge. Therefore, recharge from the Guadalupe River Basin was not considered in the lumped parameter model and only eight sub-basins losing their

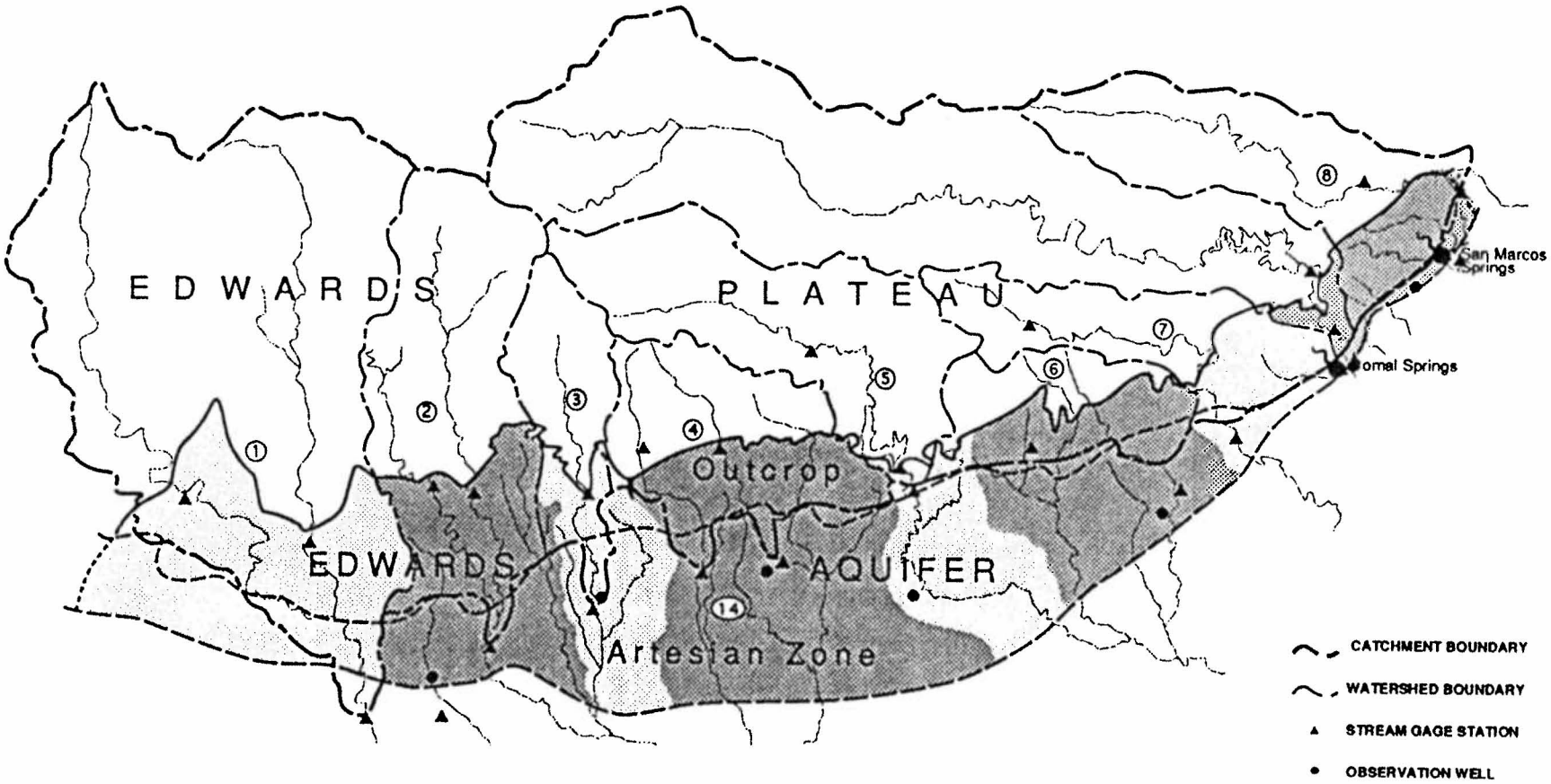

Figure 5a. Delineation of sub-basins for the Edwards Aquifer

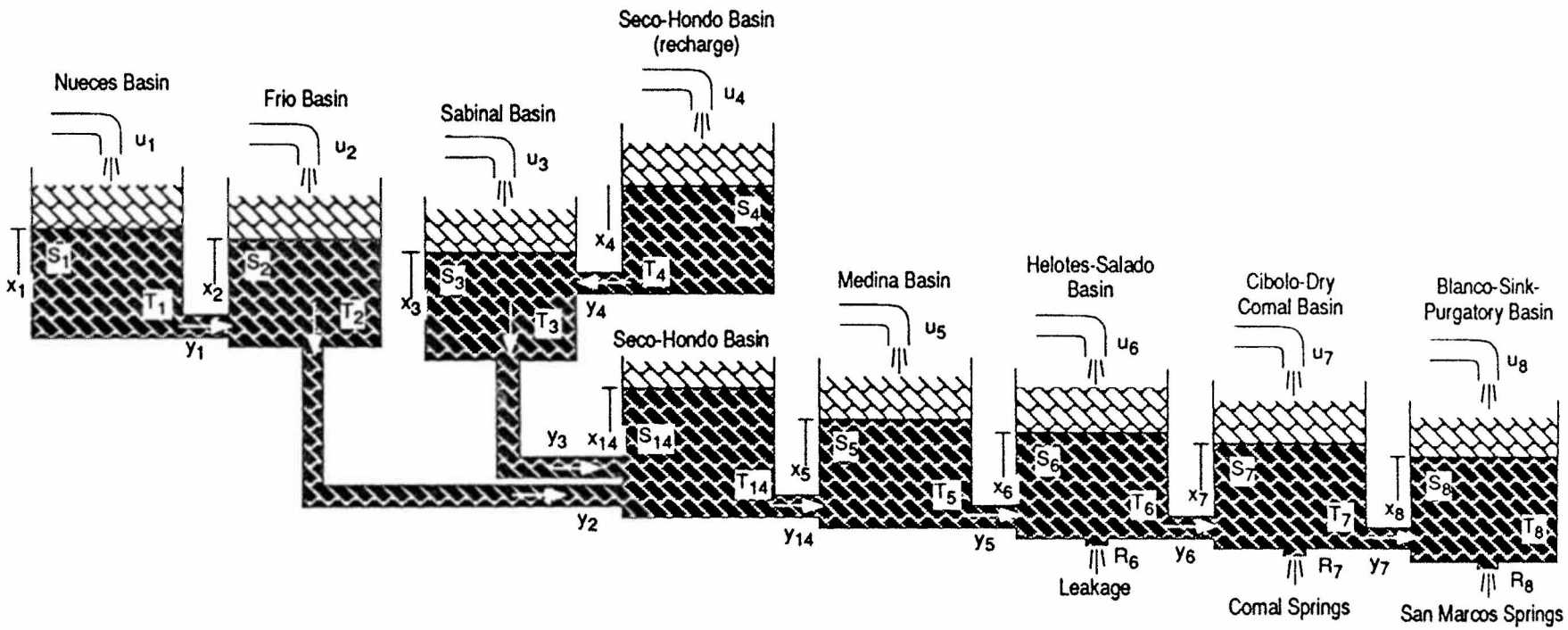

Figure 5b. The conceptual tank model for the Edwards Aquifer

Table 2 Lists of sub-basins and their associated observation wells

Sub-Basin	Upper Gage	Lower Gage	Observation Well
1 Nueces River Basin	08190500 08190000	08192000	YP 69-50-302 (H-5-1)†
2 Frio River Basin	08196000 08195000	08197500	YP 69-43-804
3 Sabinal River Basin	08198000	08198500	YP 69-45-401 (I-4-4)
4 Seco-Hondo Creek Basin-Upper	08201500 08200000	08202700 08200700	
14 Seco-Hondo Creek Basin-Lower	N/A	N/A	TD 69-47-302 (I-3-148)
5 Medina River Basin	08179500	N/A	TD 68-41-301 (J-1-82)
6 Helotes-Salado Creek Basin	08181400	08178700	AY 68-37-203 (J-17)
7 Cibolo-Dry Comal Creek Basin	08183900	08185000	DX 68-23-302 (G-49)
8 Alligator-York-Purgatory-Sink Creek-Blanco River Basin	08171000	08171300	LR 67-09-110

† Old well number

water as recharge to the aquifer were conceptualized. Figure 5a delineates those sub-basins with their labels, associated gaging stations, and representative observation wells listed in Table 2. All basins have the same general direction of groundwater flow, i.e. flowing from the recharge area to the underground outlet. Due to effects of the Knippa Gap on the flow pattern, the Seco-Hondo Creek Basin is subdivided into upper and lower sub-basins. The upper basin receives all the basin recharge while the lower basin (14) serves as a main supply line where the groundwater is transferred and pumped.

Each basin is conceptually represented by a tank in which the flow can be described by equation (16). Thus, the Edwards Aquifer conceptual model can be portrayed as a series of connected tanks assembled according to the aquifer general flow pattern. The current configuration, as shown in Figure 5b, considers only two major springs and one area of leakage. The system of ODE's describing the model has the form of equation (5) with their parameters derived following equations (10)-

(15). Flows at Comal and San Marcos Springs are determined using linear relationships between springflows and water levels in the nearby observation wells.

Computer Model Algorithm

There are two primary parameters in the tank model, namely the storage and the transmissivity related parameters. The former parameter is associated with the tank properties while the latter is dependent on the link characteristics. A tank can have more than one link to represent boundary conditions, leakage, and springflow in addition to the underflow to the nearby sub-basin. Consider the ODE similar to equation (16) for the middle leaky tank in a series of three connected tanks as shown in Figure 6,

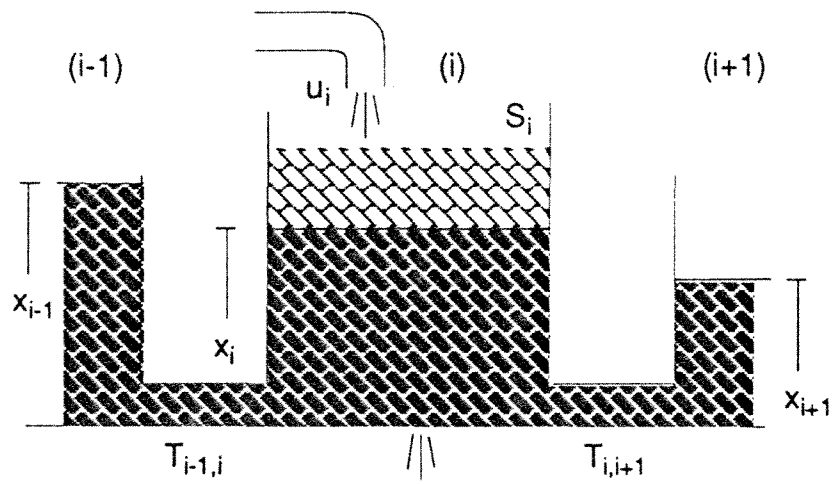

Figure 6 A tank model with multiple links as boundary conditions, springs, and leakage

$$\frac{d}{dt} x_i = \frac{1}{S_i}\left[(x_{i-1}-x_i)\, T_{i-1,i} + (x_{i+1}-x_i)\, T_{i+1,i} + (x_L-x_i)\, T_L\right] + \frac{1}{S_i} u_i \,, \qquad (17)$$

where i-1,i, and i+1 are the indices for the upstream, the middle, and the downstream tanks, respectively, (i-1,i) and (i,i+1) are the link indices, and L is the leakage index. If link (i-1,i) is a boundary, one can set $x_{i-1} = \alpha_i + \beta_i x_i$ for a mixed boundary condition while $\alpha_i = 0$ and $\beta_i = 0$ gives constant flux and constant head boundary conditions, respectively. If link (i,i+1) represents springs, the relationship between springflow and water level can be used to determine flow through the link.

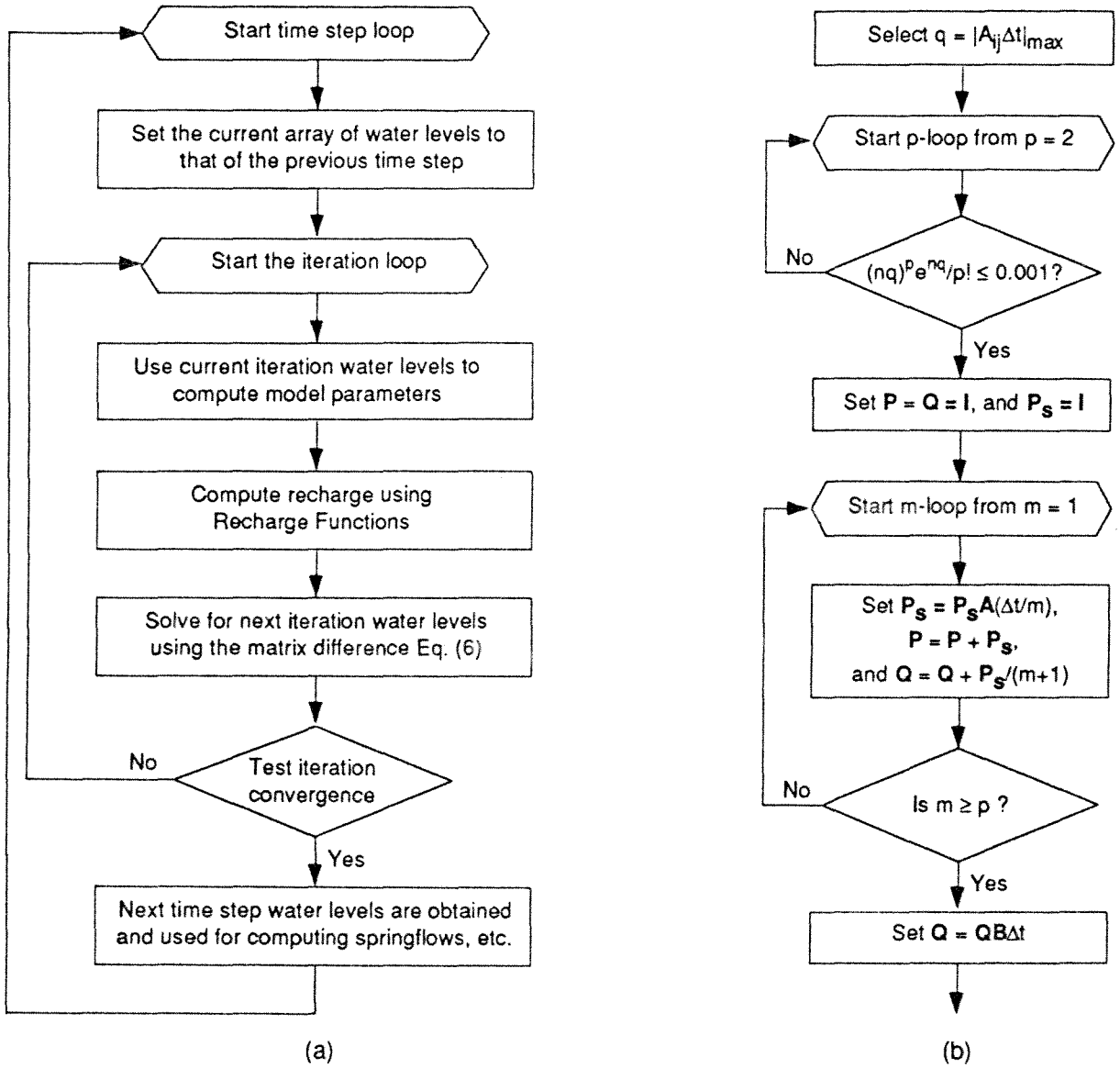

Figure 7. Flow charts for (a) iterative procedure for solving a nonlinear system, (b) Paynter's algorithm for obtaining **P** and **Q**

For a linear relationship, e.g. springflow = $\alpha_i + \beta_i x_i$, the second term in the brackets of equation (17) should be replaced by $\alpha_i + \beta_i x_i$. Similarly, leakage can be treated as a link, and x_L and T_L become constants representing the adjacent aquifer water levels and the leakage parameter, respectively. Here, the leakage parameter is defined as the product of the hydraulic conductivity of the aquitard and the leakage area divided by the aquitard thickness.

Since the model parameters are a function of state variables or water levels, the resulting model governing equations are nonlinear. Therefore, the solution

given in equation (9) for the linear parameter model can not be applied directly. An iterative procedure based on the linear solution is devised to solve the nonlinear model as shown on Figure 7. At the beginning of the iteration process, the model parameters are computed using the previous time-step water levels and the solution equation (6) is applied. As iterations proceed, the parameters are recomputed using water levels obtained from the previous iteration. For the storage parameter function S(x), its value is evaluated using the time-average water levels. However, the aquifer thickness used for evaluating the transmissivity parameter function T(x) is the spatial and temporal average value between the linked basins over the consecutive time-steps. The iteration process is converged when the sum of changes in water levels between two consecutive iterations is less than the preset tolerant limit. Then, water levels for the next time-step are obtained and used for computing other output, such as springflows, leakage, and basin underflows. The computation advances to the next time-step and the iteration process is repeated.

To solve equation (6), the matrix exponent equation (8) as well as system parameter **P** and **Q** must be evaluated analytically or numerically. We chose a numerical solution using the algorithm suggested by Paynter (see Takahashi, et al., 1972). The algorithm shown in Figure 7b is simply a series expansion of equation (8) to the pth term, in which p can be determined from the following relationship,

$$\frac{1}{p!}(nq)^p e^{nq} = 0.001, \tag{18}$$

where n is the order of the system, $q = \max|A_{ij}\Delta t|$, and A_{ij} is an element of the **A** matrix.

Flow loss and Recharge Function

There are two existing methods for calculating recharge to the Edwards Aquifer, i.e. the methods used by the USGS and HDR Engineering, Inc. Both methods are inappropriate to implement in the current modeling for several reasons. First, they require lower gage flow data which are unobtainable during predictive simulation. Second, in addition to streamflow data, they both use rainfall data which the current model intends to avoid to keep the model input simple. They also do not consider the influence of groundwater levels on recharge capacities. Despite their complexity, the methods have not proved advantageous over a less complex method as will be discussed in the following.

To be able to project recharge for predictive simulation, a relationship between estimated losses and the upper gage flows for each sub-basin must be established from a flow loss analysis. In some cases, the relationship must also account for the effect of groundwater level, especially for the sub-basins with shallow water tables. This relationship, which is referred to as a recharge function, is used by the model to calculate the sub-basin recharge given a streamflow at the upper gage and a groundwater level. The function is empirically developed based on the regression analysis of estimated losses, observation well data, and the surface inflow above the lower gage computed from the gaged flow data. In sub-basins where stream gage data are not available, inflows are determined by interpolating from adjacent river basins.

The estimated losses are obtained by simplifying the USGS method of recharge calculation. Per-unit-area runoffs from the intermediate drainage area between the upper and lower gages and from the drainage area above the upper gage are assumed to be the same. The water balance for the river stretch crossing the recharge zone can be expressed as:

$$\text{Loss} = Q_U - Q_L + Q_I \; ; \qquad Q_I = Q_U \frac{A_I}{A_U} , \tag{19}$$

where Q_U and Q_L are the monthly streamflows at the upper and lower gages, respectively. Q_I is the surface runoff in the drainage area between gages, and A_U and A_I are drainage areas above the upper gage and between upper and lower stream gages. It is more convenient to express a loss in terms of a Loss Ratio (LR), which is defined as the loss per the total surface inflow above the lower stream gage or,

$$\text{LR} = \frac{\text{Loss}}{\text{Inflow}} = 1 - \frac{Q_L}{Q_U + Q_I} \tag{20}$$

The ratios are then plotted against monthly inflows from the upper gage and average water levels from previous months. Figures 8-17 show the plots of each sub-basin except the Medina where recharge is determined based on the Medina reservoir content. Since only the Nueces and Sabinal Sub-Basins show the effects of water levels on recharge, the plots of LR versus water level for other sub-basins are not depicted. Recharge functions for each sub-basin are determined by analyzing the plots using linear regression models. Results of analyses are given below, in

which the loss, inflow, and recharge capacity (RC) are given in thousand ac-ft and the water level (WL) is in feet above the mean sea level (MSL).

Nueces River Basin

The aquifer under this basin is shallow. Figure 8 illustrates a line where losses equal to the capacity. As expected, the plot in Figure 9 reveals a close relationship between LR and water level. The basin losses are also believed to be controlled by a recharge capacity, a physical limitation of the recharge features. In general, the recharge function can be expressed as follows:

$$\text{Loss} = \min(\text{RC}, \text{Inflow} \times \text{LR}) \tag{21}$$

$$0 \leq \text{LR} = 1 - \left[\frac{k}{(H_m - \text{WL})}\right]^m \leq 1 \tag{22}$$

where constants k = 37.5902 ft; m = 3.6814; H_m = 927.65 ft MSL; and the recharge capacity, RC = 29.0 × 10^3 ac-ft.

Frio River Basin

The correlation of LR and inflow can be observed in the semi-log plot of Figure 10. However, the plot in Figure 11 shows no significant correlation between LR and water level even though the basin is in the shallow aquifer region. This may partly be due to the poor water level records used in the analysis. The recharge function for this basin can be given as

$$\text{Loss} = \text{Inflow} \times \text{LR} \tag{23}$$

$$0 \leq \text{LR} = \frac{\ln(\text{Inflow}) - b}{a} \leq 1 \tag{24}$$

where parameters a and b are -1.72581 and 4.95753, respectively.

Sabinal River Basin

The LR-inflow plot (Figure 12) seems to follow the similar pattern of the one in the Frio River Basin. Losses in this basin show a weaker correlation to groundwater level (Figure 13) than those in the Nueces. The recharge is determined from both water levels and inflows by the following relationships

$$\text{Loss} = \text{Inflow} \times \text{LR} \tag{25}$$

$$0 \leq \text{LR}' = \frac{\ln(\text{Inflow}) - b}{a} \leq 1 \tag{26}$$

$$\text{LR} = \begin{cases} 1 - \dfrac{k}{(H_m - \text{WL})} & \text{if LR}' > 0.9 \text{ and WL} < 824 \\ \text{LR}' & \text{else} \end{cases} \tag{27}$$

where parameters a and b are -2.06389 and 3.63713, respectively, and constants k = 4.67863 ft; and H_m = 870 ft MSL.

Seco-Hondo Creeks Basin

The loss function in this basin is presumed to be similar to the Frio River Basin. Based on the plot in Figure 14, the recharge function can be given as:

$$\text{Loss} = \text{Inflow} \times \text{LR} \tag{28}$$

$$0 \leq \text{LR} = \frac{\ln(\text{Inflow}) - b}{a} \leq 1 \tag{29}$$

where parameters a and b are -2.77614 and 5.36413, respectively.

Helotes-Salado Creek Basin

The only available gaging stations are the upper gage on Helotes Creek and the lower gage on Salado Creek. Interpolation of runoff from the nearby streams were attempted to obtain adequate flow data for stream loss analysis. The procedure did not provide good recharge estimates as the plot of LR versus Inflow failed to show correlation (Figure 15). Thus, the recharge function is formulated assuming that the basin inflow losses are the same rate as losses of the nearby Cibolo Creek Basin. Hence

$$\text{Loss} = \text{Inflow} \times \text{LR}_{\text{cibolo}} \tag{30}$$

Cibolo-Dry Comal Creek Basin

The recharge function for the basin is determined from losses in the Cobolo and Cry Comal Creeks at different loss rates. Runoff in the Dry Comal Creek drainage area is assumed to lose all water to the aquifer up to its recharge capacity.

The LR in the Cibolo Creek is derived from the plot (Figure 16) using linear regression on the semi-log scale. The basin recharge function becomes:

$$\text{Loss} = [\text{Inflow} \times \text{LR}]_{\text{cibolo}} + \min\,[\text{RC},\text{Inflow}]_{\text{drycomal}} \tag{31}$$

$$0 \le \text{LR}_{\text{cibolo}} = \frac{\ln[\text{Inflow}]_{\text{cibolo}} - b}{a} \le 1 \tag{32}$$

where parameters a and b are -1.84034 and 4.44984, respectively.

Blanco River Basin

The LR for the Blanco River Basin showed a strong presence of the recharge capacity. All data points with inflows greater than the RC are fallen along the line LR = RC/Inflow, as shown in Figure 17. A weak dependency of the LR to groundwater level is also observed. However, the analysis was unable to provide a concrete functional relationship. Hence, the recharge function for the basin can be given simply as:

$$\text{Loss} = \min\,[\text{RC},\text{Inflow}] \tag{33}$$

where RC = 1.331×10^3 ac-ft.

Medina River Basin

Recharge from the basin largely comes from seepage losses of the Medina Lake. The procedure used to estimate the losses follows Lowry (1955) who constructed correlation curves between reservoir seepage losses and the monthly average reservoir contents. The procedure is simplified by replacing the curves with the following function:

$$\text{Loss} = \frac{b}{\left[\dfrac{a}{V - y_p} - 1\right]^n} + x_p \tag{34}$$

where V is the reservoir content in thousand ac-ft, parameters a and y_p are 263.8 and 1.533 thousand ac-ft, respectively, and constants b = 2.99645 and n = 0.29455. The loss constant x_p is equal to 1.0 and 3.38084 thousand ac-ft for falling and rising of reservoir stages, respectively. The curves are plotted as shown in Figure 18.

Adjacent Areas

Additional recharge from adjacent areas of the above sub-basins is calculated from the recharge of those basins. Except the area adjacent to the Blanco River Basin, all losses from other adjacent areas are assumed to be proportional to their corresponding basin losses. Losses from the area adjacent to the Blanco River Basin is thought to be controlled by the recharge capacity at the same magnitude as Dry Comal Creek.

Figure 19 compares the estimated recharge by the USGS and estimated recharge using the recharge functions developed in this study.

Pumpage Estimation

Monthly pumpage data used in the recent TWDB simulation model was adjusted for each sub-basin. The TWDB simulation cell data was grouped into sub-basins by encoding a basin cell map. The monthly data was available only from 1978 to 1989. Monthly pumpage data by basin outside this period was estimated using USGS annual county pumpage data and pumpage distribution coefficients derived for each basin. First, annual county pumpage data was converted into annual basin pumpage data according to the percentage of the surface area of the basin in each county. Then, the annual pumpage for each basin was multiplied by the pumpage distribution coefficients to estimate monthly pumpage within each basin for the periods of missing pumpage data. The pumpage distribution coefficients are the average ratios of monthly to annual pumpage within each basin computed from adjusted TWDB data shown in Figures 20 to 27. Note that irrigation pumpage in the western basins are season dominated in contrast to municipal pumpage in the eastern basins.

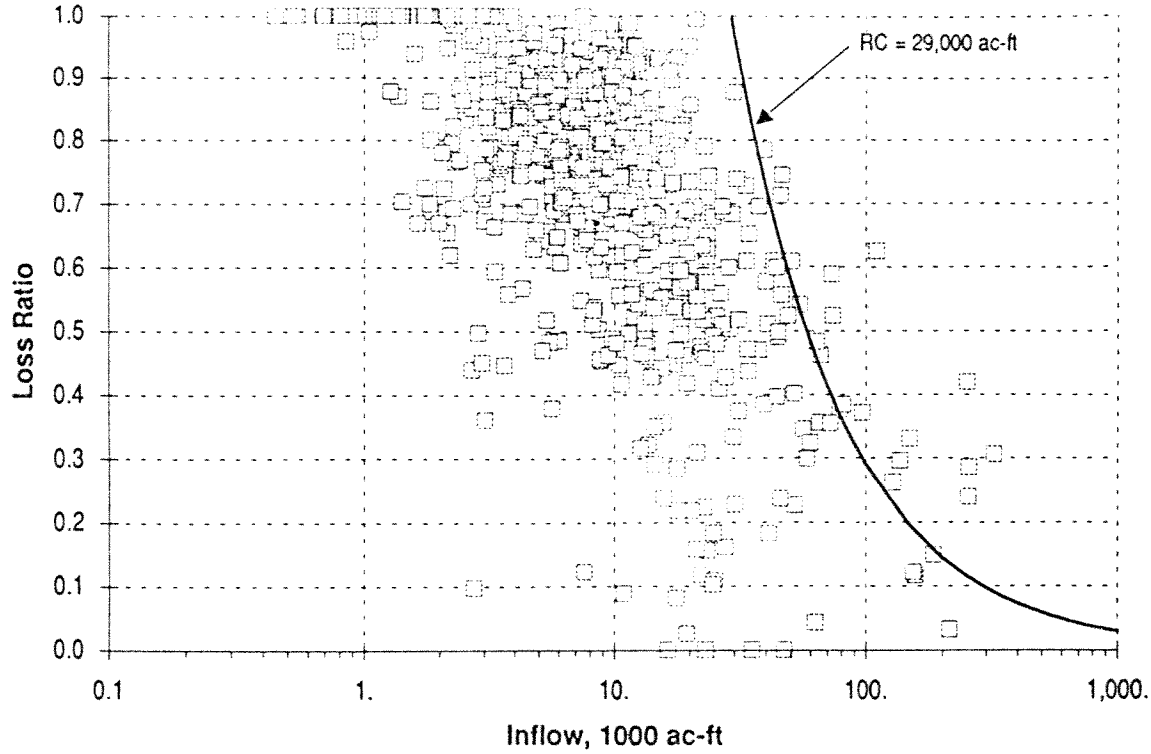

Figure 8. A plot of loss ratio versus inflow in the Nueces River Basin

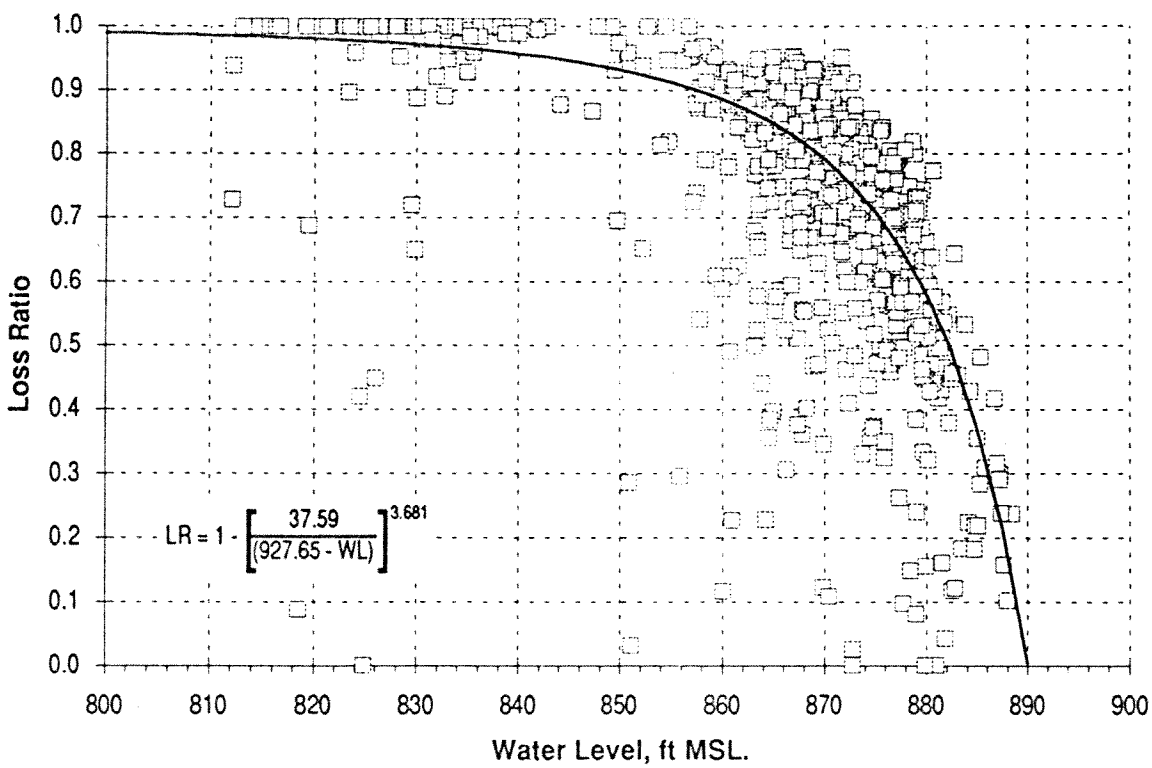

Figure 9. A plot of loss ratio versus water level in the Nueces River Basin

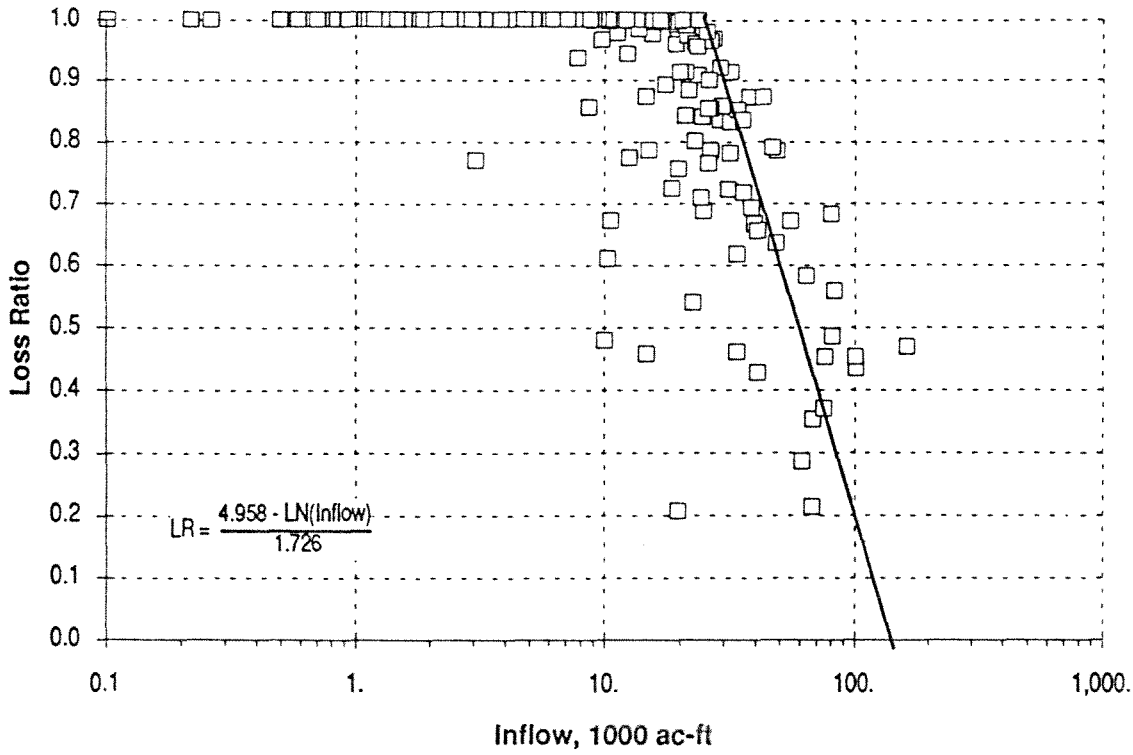

Figure 10. A plot of loss ratio versus inflow in the Frio River Basin

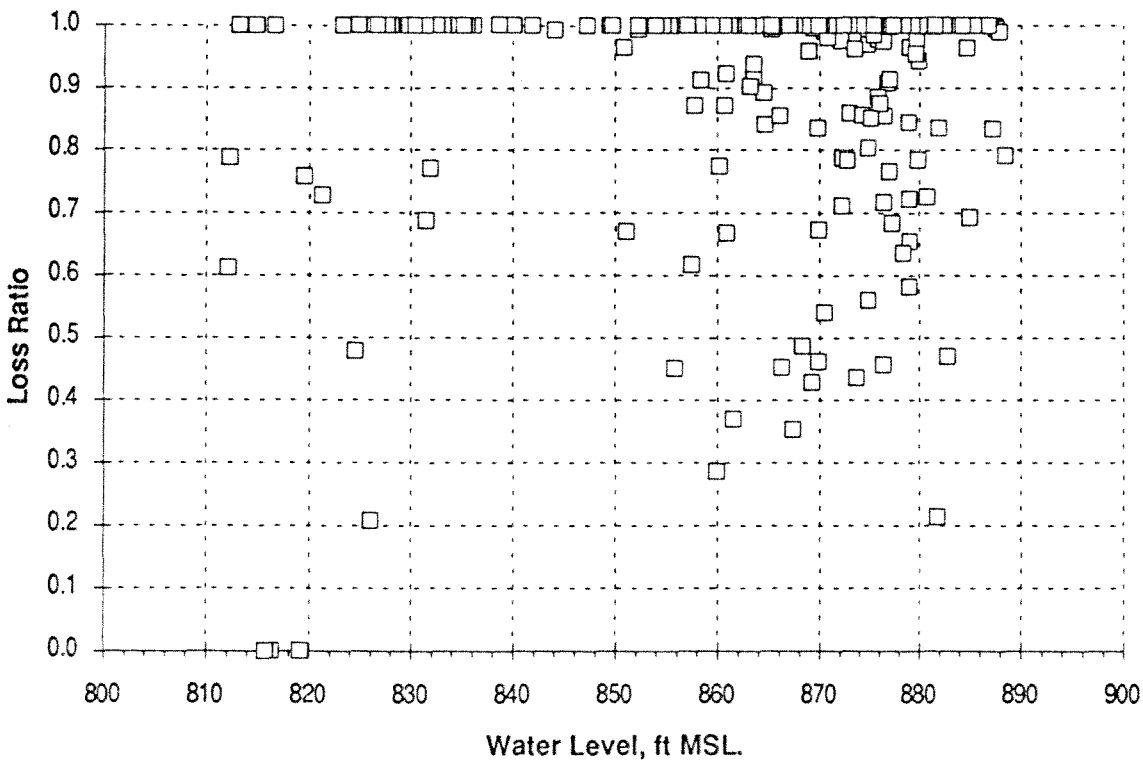

Figure 11. A plot of loss ratio versus water level in the Frio River Basin

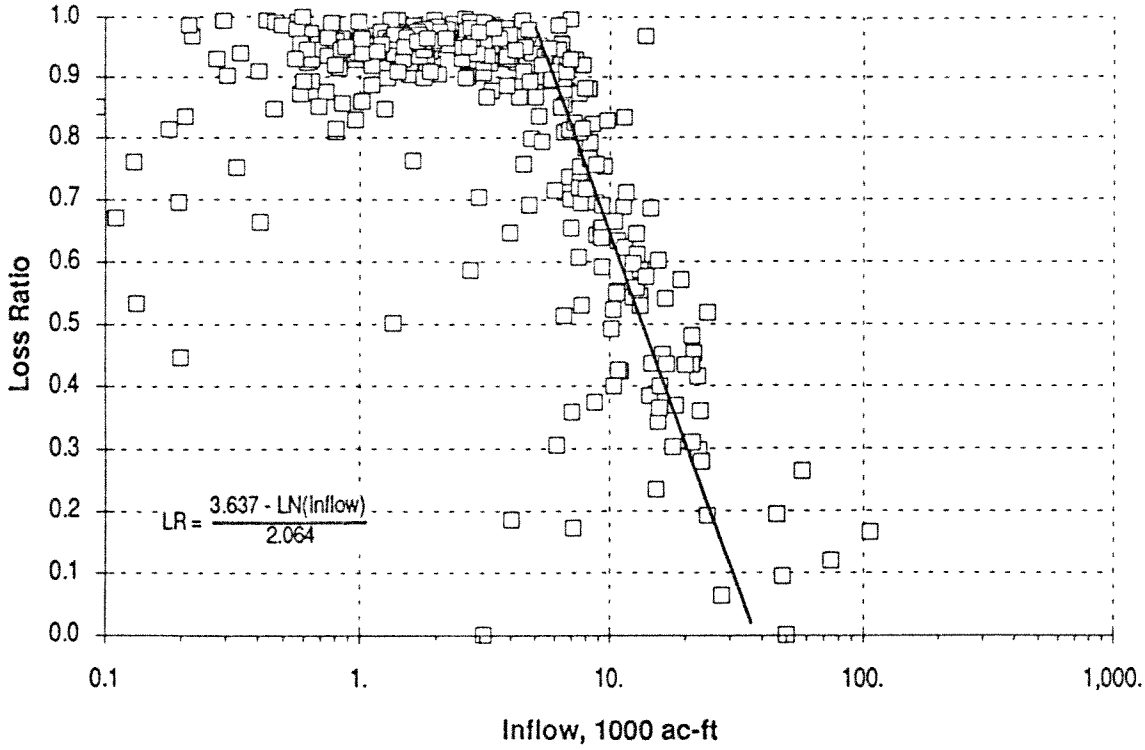

Figure 12. A plot of loss ratio versus inflow in the Sabinal River Basin

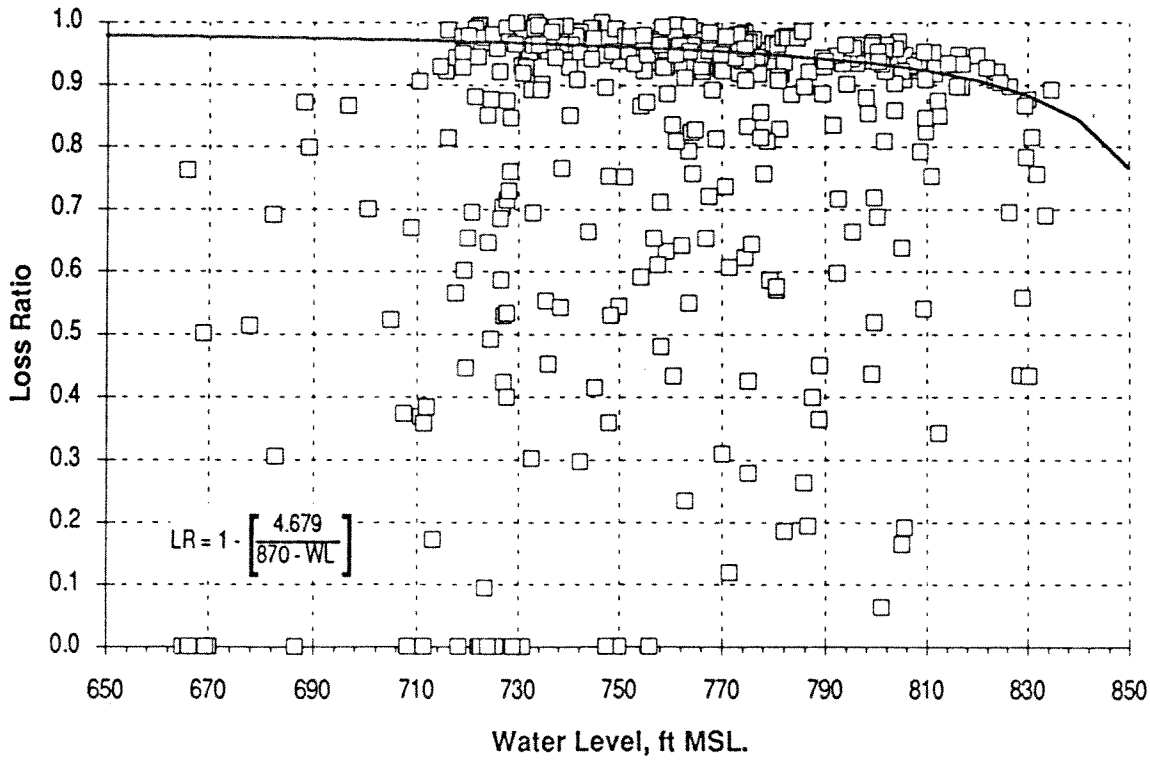

Figure 13. A plot of loss ratio versus water level in the Sabinal River Basin

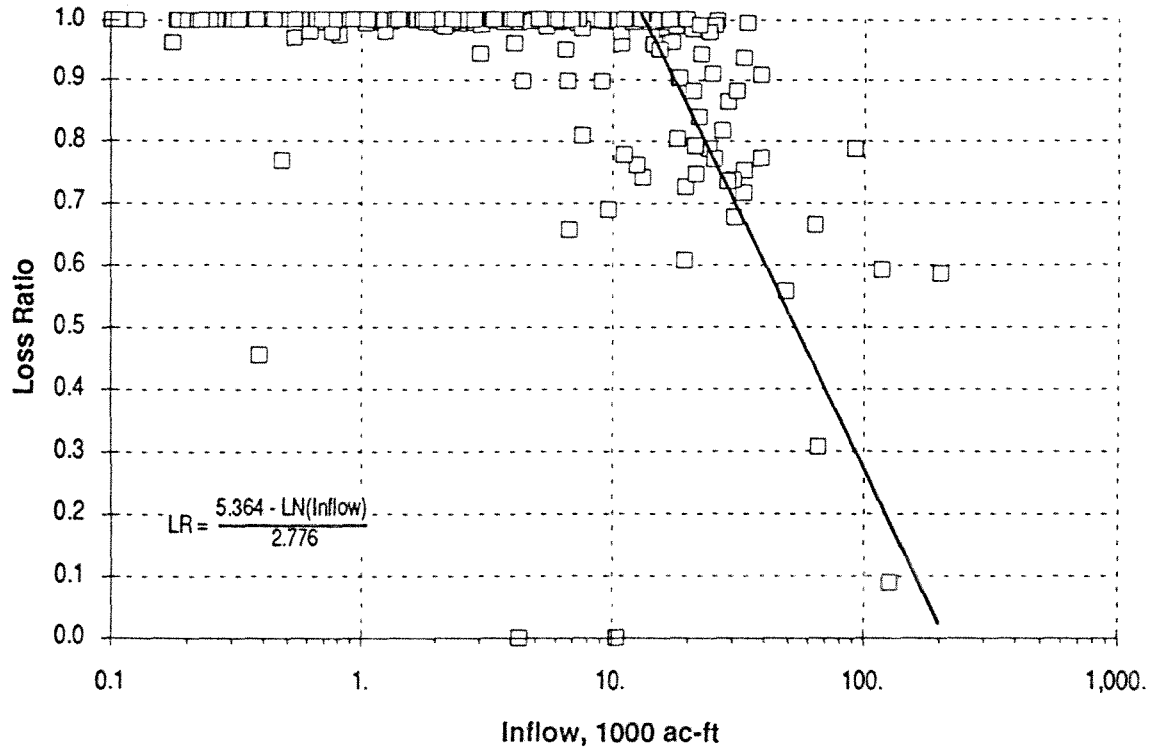

Figure 14. A plot of loss ratio versus inflow in the the Seco-Hondo Creek Basin

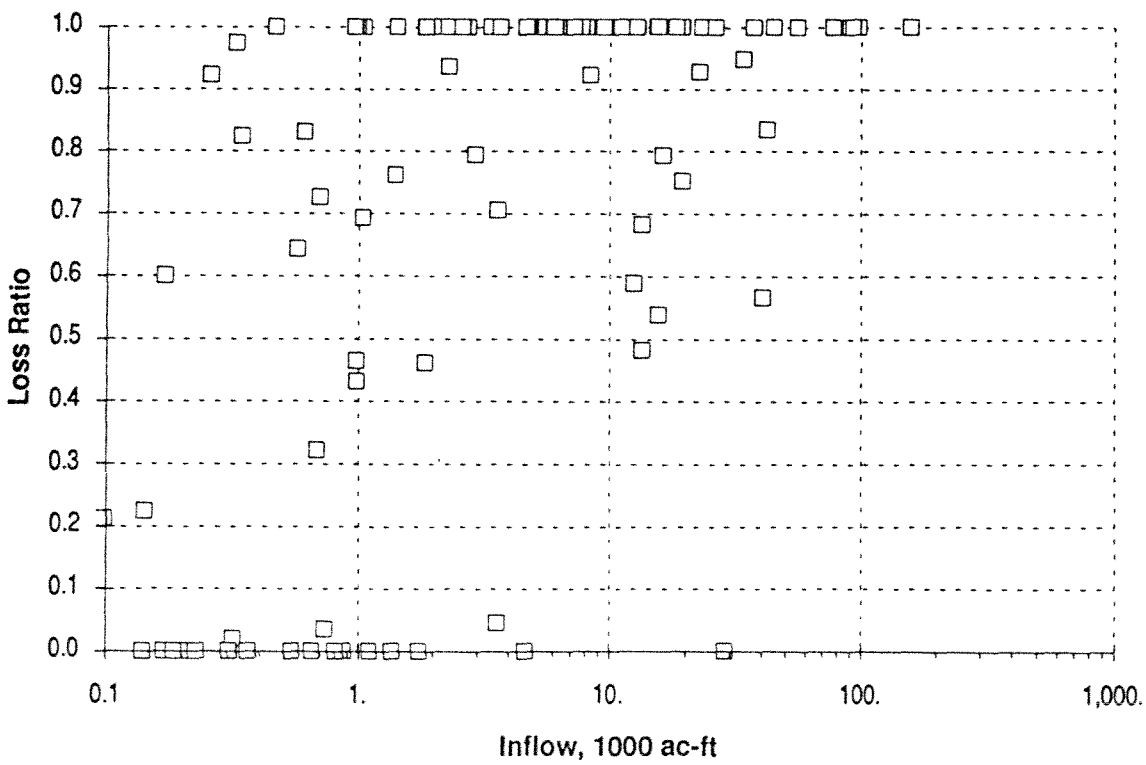

Figure 15. A plot of loss ratio versus inflow in the Helotes-Salado Creek Basin

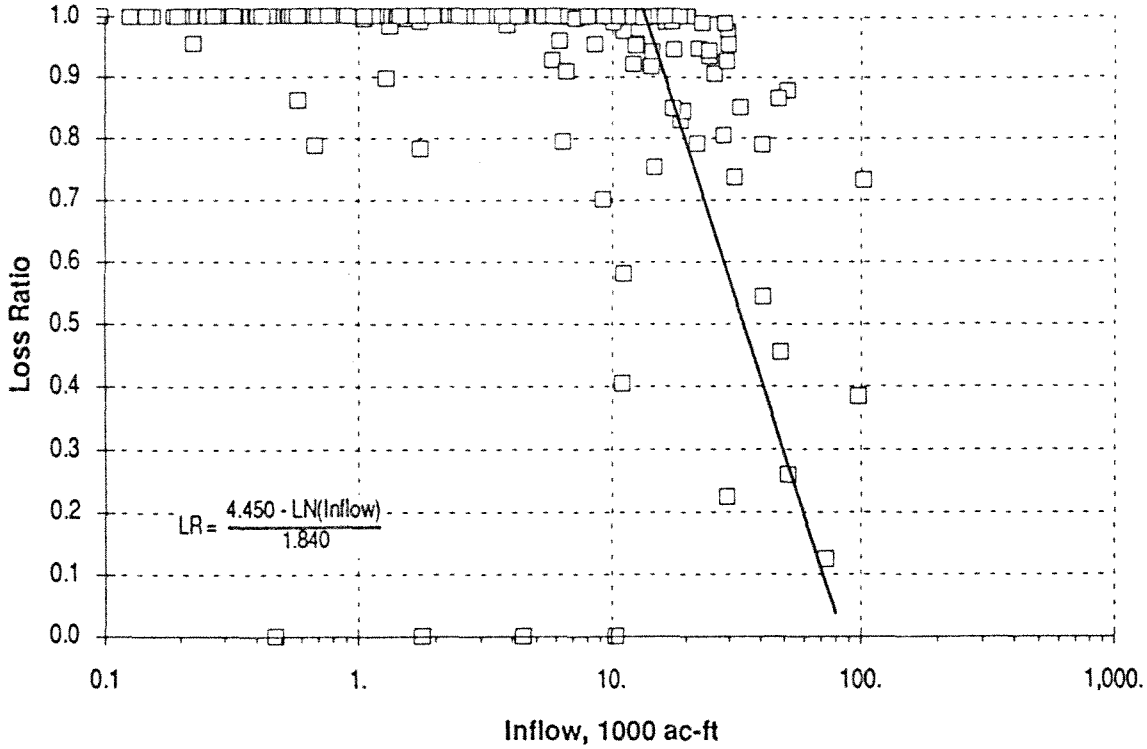

Figure 16. A plot of loss ratio versus inflow in the Cibolo-Dry Comal Creek Basin

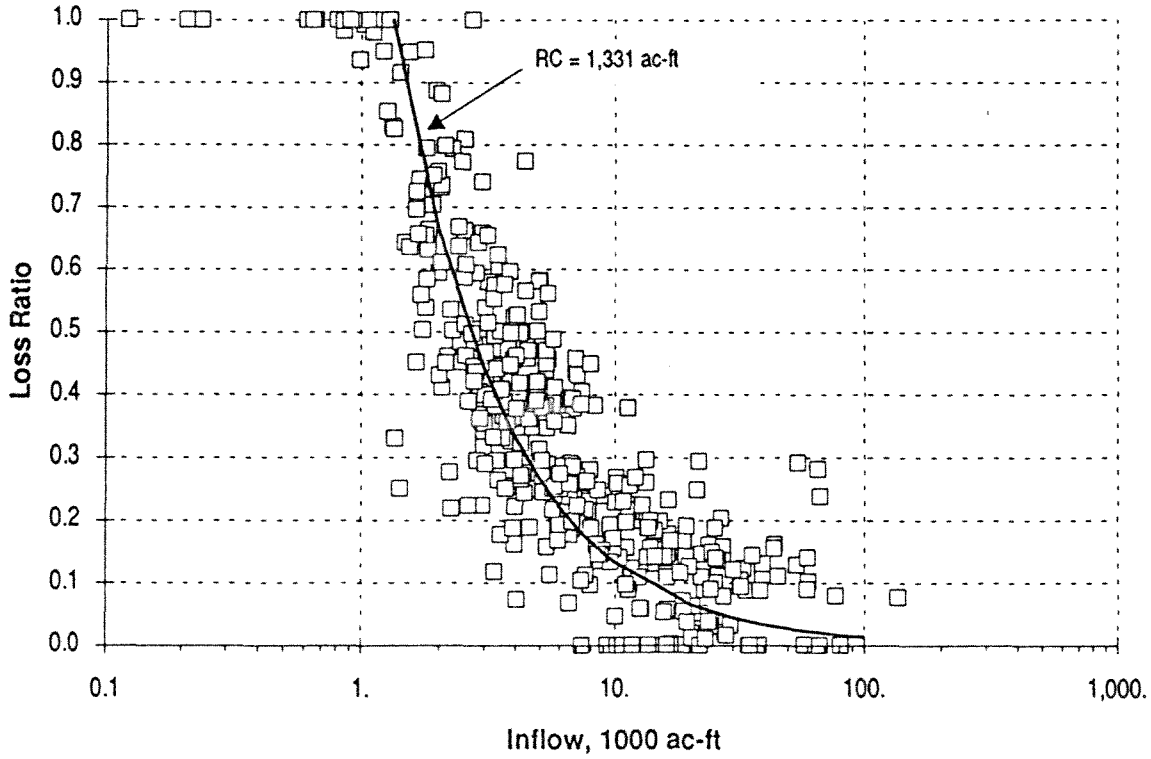

Figure 17. A plot of loss ratio versus inflow in the Blanco River Basin

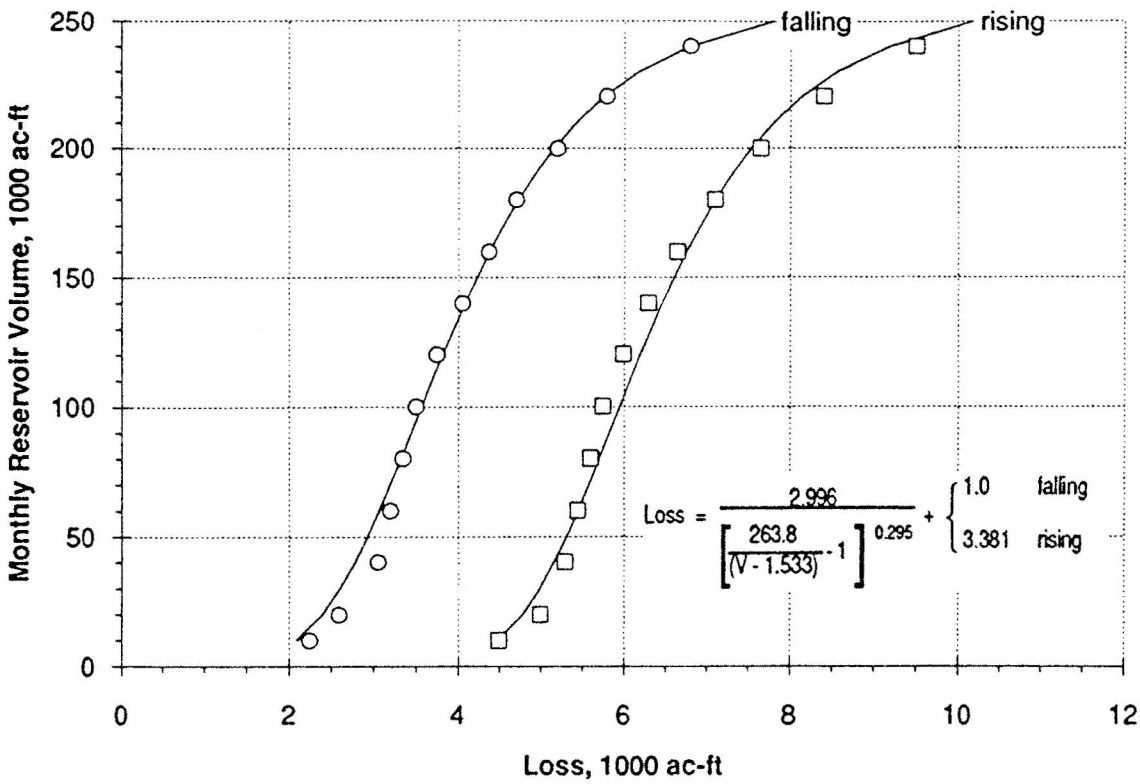

Figure 18. The loss curves for estimating recharge from Medina Reservoir

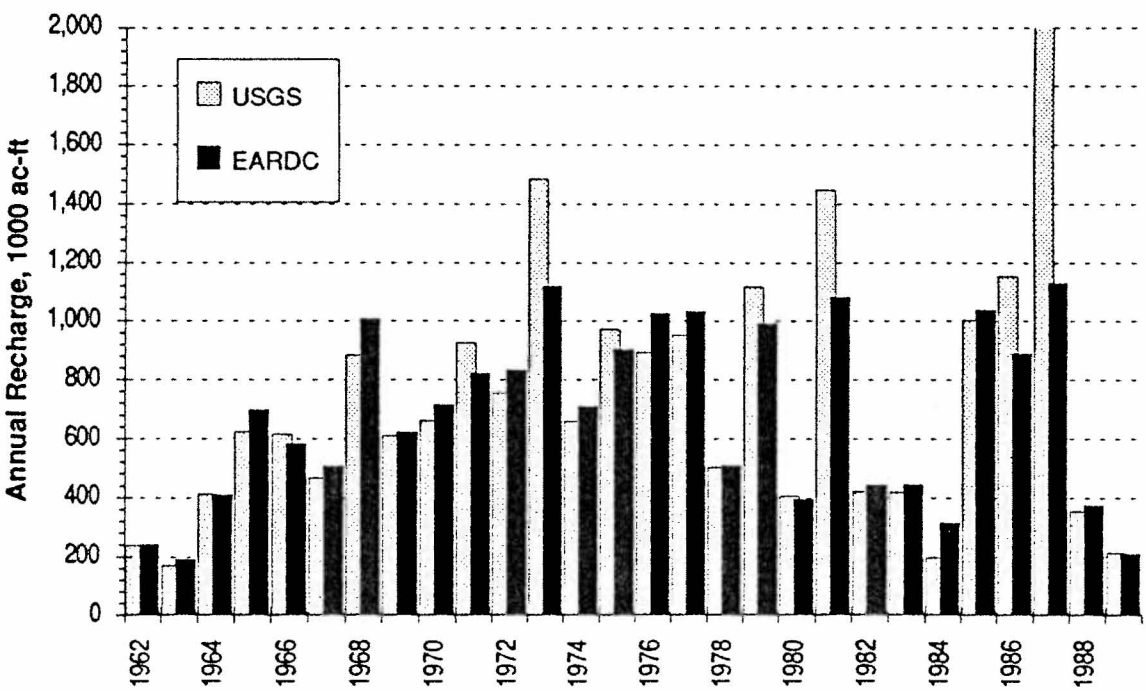

Figure 19. Comparison of recharge estimates by the USGS and the recharge functions developed by this study

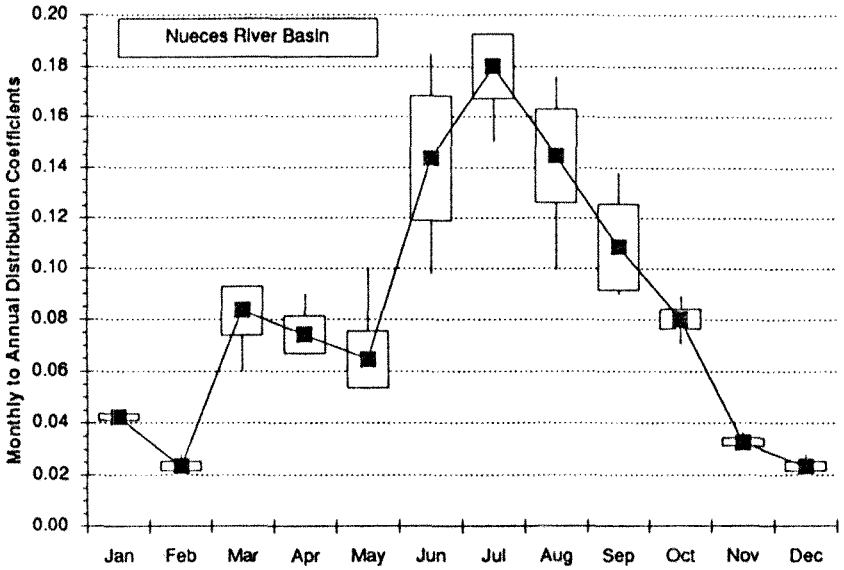

Figure 20. Nueces River Basin pumpage distribution coefficients

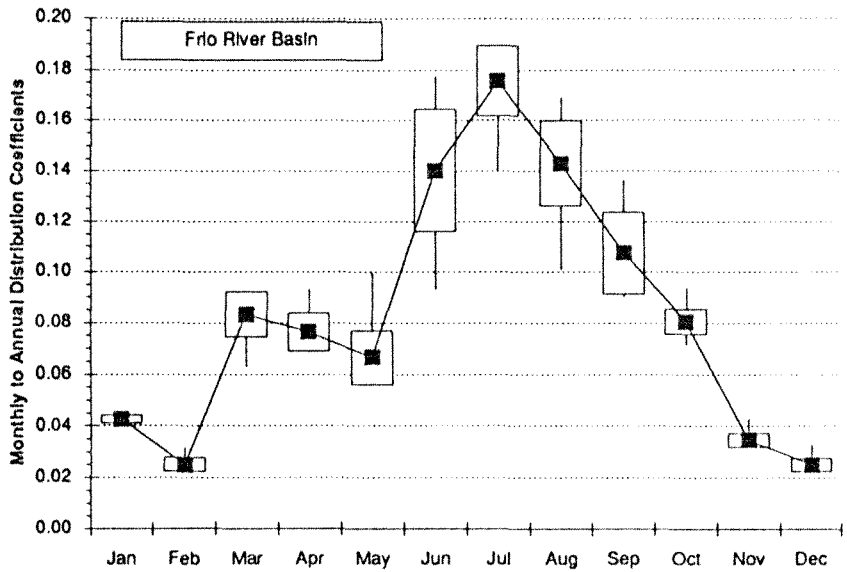

Figure 21. Frio River Basin pumpage distribution coefficients

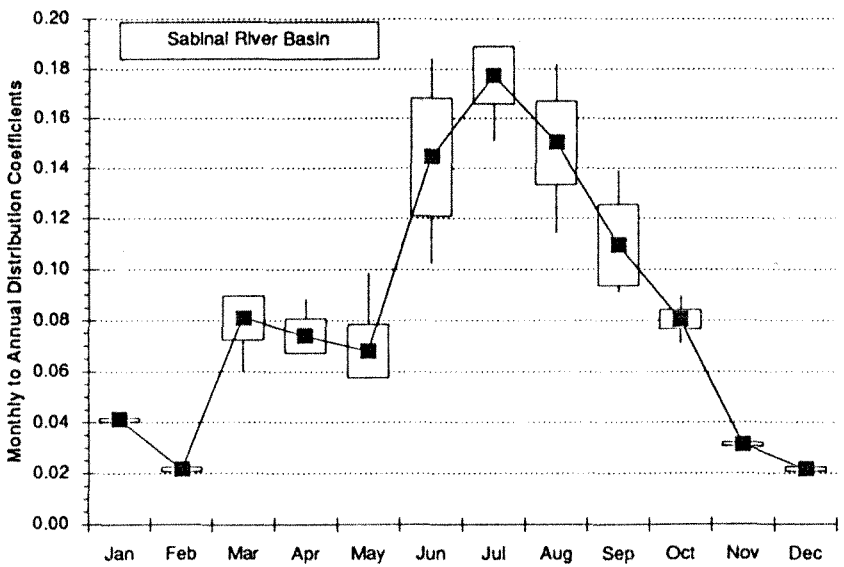

Figure 22. Sabinal River Basin pumpage distribution coefficients

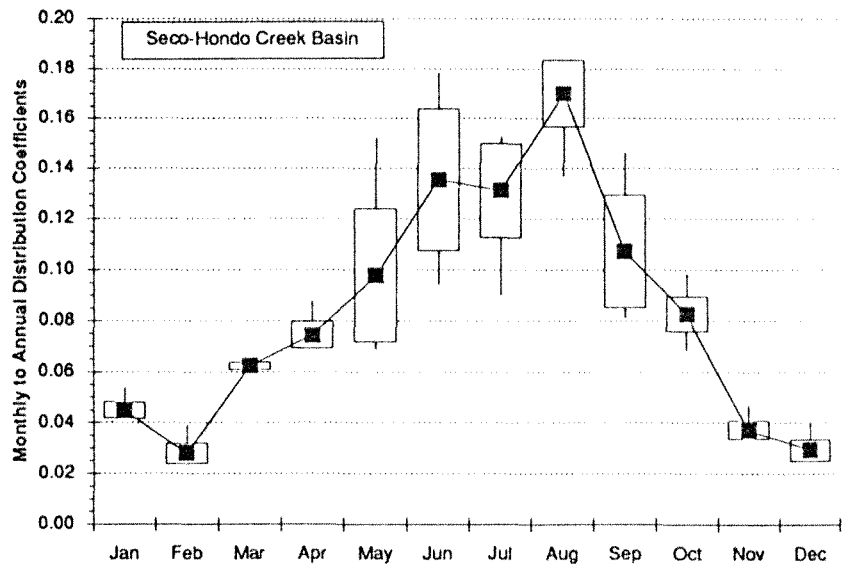

Figure 23. Seco-Hondo Creek Basin pumpage distribution coefficients

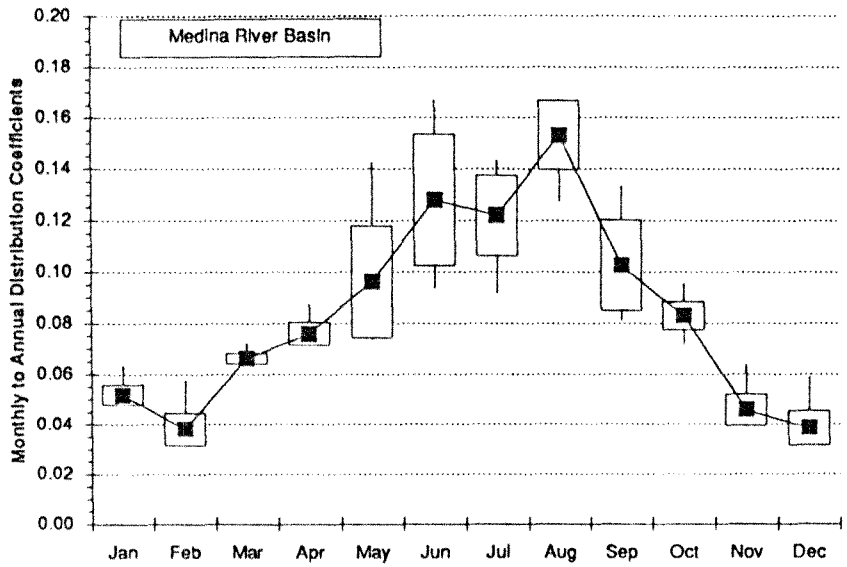

Figure 24. Medina River Basin pumpage distribution coefficients

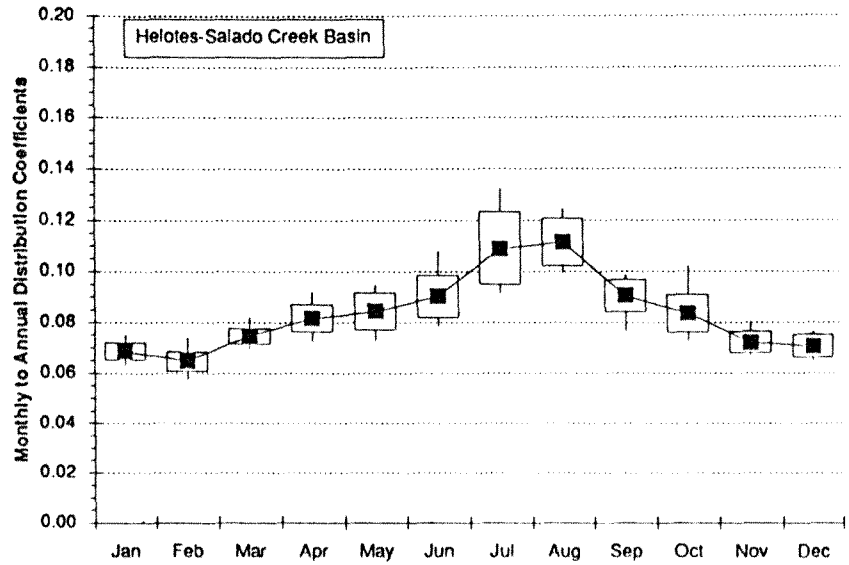

Figure 25. Helotes-Salado Creek Basin pumpage distribution coefficients

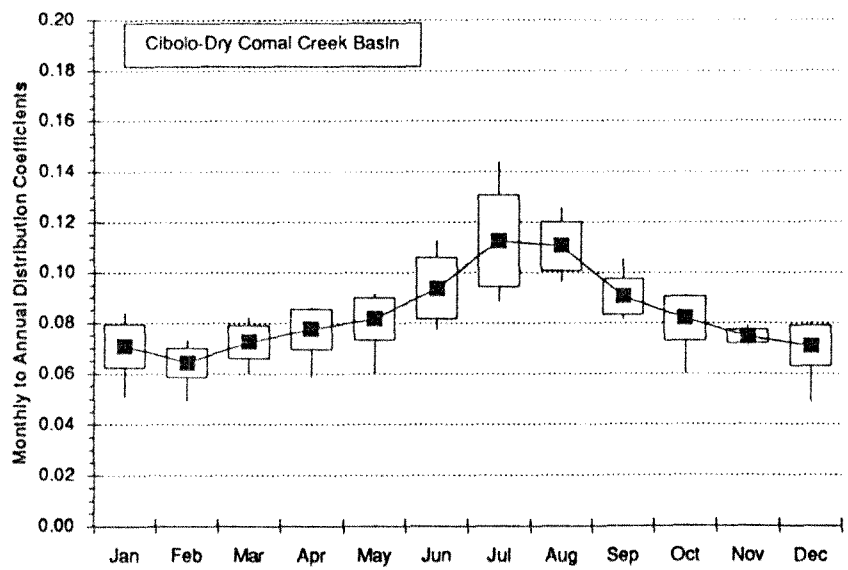

Figure 26. Cibolo-Dry Comal Creek Basin pumpage distribution coefficients

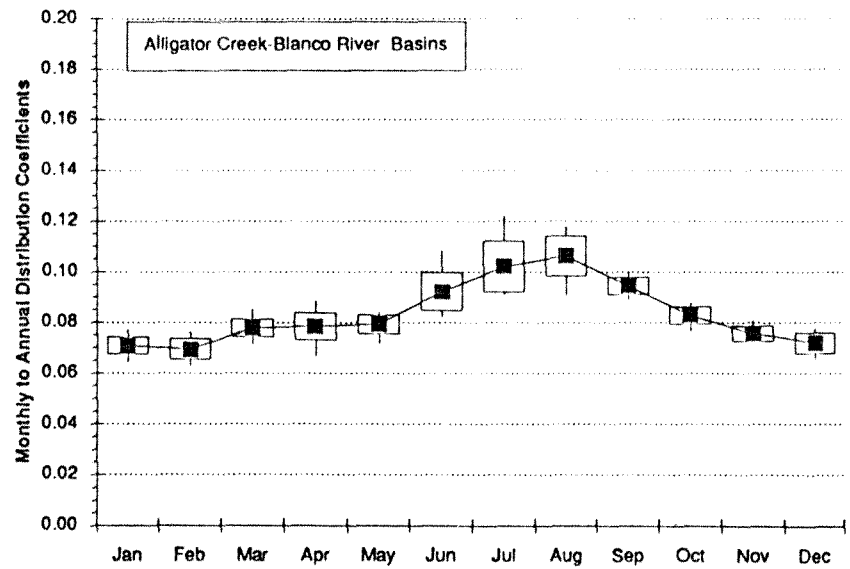

Figure 27. Alligator Creek-Blanco River Basin pumpage distribution coefficients

MODEL VERIFICATION AND CALIBRATION

Before the model can be used, its physical and flow parameters had to be calibrated and verified with two separate data sets. Stream flow, water level, and pumpage data are the only time dependent inputs and are divided into two sets, January 1975 to September 1990 and March 1962 to December 1974. The former were used in calibration while the latter were used for validation. Conventional procedures for model calibration use a trial and error method in accordance with a sensitivity analysis. In this study, a modern optimization procedure for model calibration was adopted. The procedure automates the trial and error process by formulating and solving a nonlinear programming problem to calibrate parameters.

Database Development

A database for the model input has been established on a microcomputer spreadsheet. Many useful features and functions in the spreadsheet, such as cell formulas, command macros, auto-update, and linking make the software very attractive for use in preparing and manipulating the model input. For instance, the software makes it more convenient to change stream-flow units or to obtain ungaged stream-flow data by interpolation. Furthermore, this model's development was geared toward using the model in a microcomputer spreadsheet.

Estimation of Parameters

The calibrating parameters include the storage related parameters in each sub-basin and the flow transmissivity related parameters in each link. Initial values of the parameters are required as a starting point in the calibration process. To estimate the initial values, relationships between the aquifer storativity versus the model storage parameter and the aquifer transmissivity versus the model flow transmissivity parameter need to be determined. By definition, the storativity, S_y, is defined as the volume of water that an aquifer releases from storage per unit surface area per unit decline in hydraulic head. Using equation (11), S_y for a sub-basin can be expressed in terms of storage parameter, S, as follows:

$$S_y = \frac{1}{A_b}\frac{d\forall}{dx} = \frac{1}{A_b}S'n(x-x_0)^{n-1} = \frac{1}{A_b}S \qquad (35)$$

where A_b is the basin surface area, and $d\forall/dx$ is the change in water storage per unit change in water level. Klemt, et al. (1978) reported the values of S_y to be 0.02 in the unconfined portion of the Edwards Aquifer and 0.0004-0.0007 in the confined. Maclay and Land (1988) suggested wider ranges of S_y, i.e., 2-20% for the unconfined and 10^{-5}-10^{-4} for the confined. For a S_y value of 0.01 or 1%, the equivalent S value in 10^3 ac-ft/ft can be computed from

$$S = 0.0064\, A_b S_y \tag{36}$$

where A_b is given in square miles and S_y is in percent. This equation is used to estimate the basin storage related parameters in which n is initially set to unity.

For transmissivity, Klemt, et al. (1978) performed pumping tests and reported the values of 0.1-0.2 M gal/ft/day (0.155-0.309 ft^2/s) in the water table zone and 10-20 M gal/ft/day (15.5-30.9 ft^2/s) in the artesian zone. Maclay and Land (1988) suggested the values are as high as 0.1-20.0 ft^2/s in the unconfined and 20-100 ft^2/s for the confined. In equation (14) we defined the flow transmissivity related parameter as $T = T'w/L$ where T' is the transmissivity. For a T' of 1 ft^2/s, the equivalent value of T in 10^3 ac-ft/ft/mo can be computed from

$$T = 0.06033 \left(\frac{w}{L}\right) T' \tag{37}$$

where w and L are in feet and T' is in ft^2/s. The equation is used to estimate the flow transmissivity related parameters for each basin. Note that the parameters used in model input and calibration are in terms of T/b where b is the basin thickness.

Other physical parameters, e.g. elevations of the top and bottom of the aquifer in each basin, are not adjusted during the calibration. Each basin value is calculated from the TWDB model input by averaging the cell values in the basin. Springflow parameters are determined from the regression analysis as shown in Figure 28.

Optimization in Calibration Process

The calibration process is automated by solving the following nonlinear programming problem ,

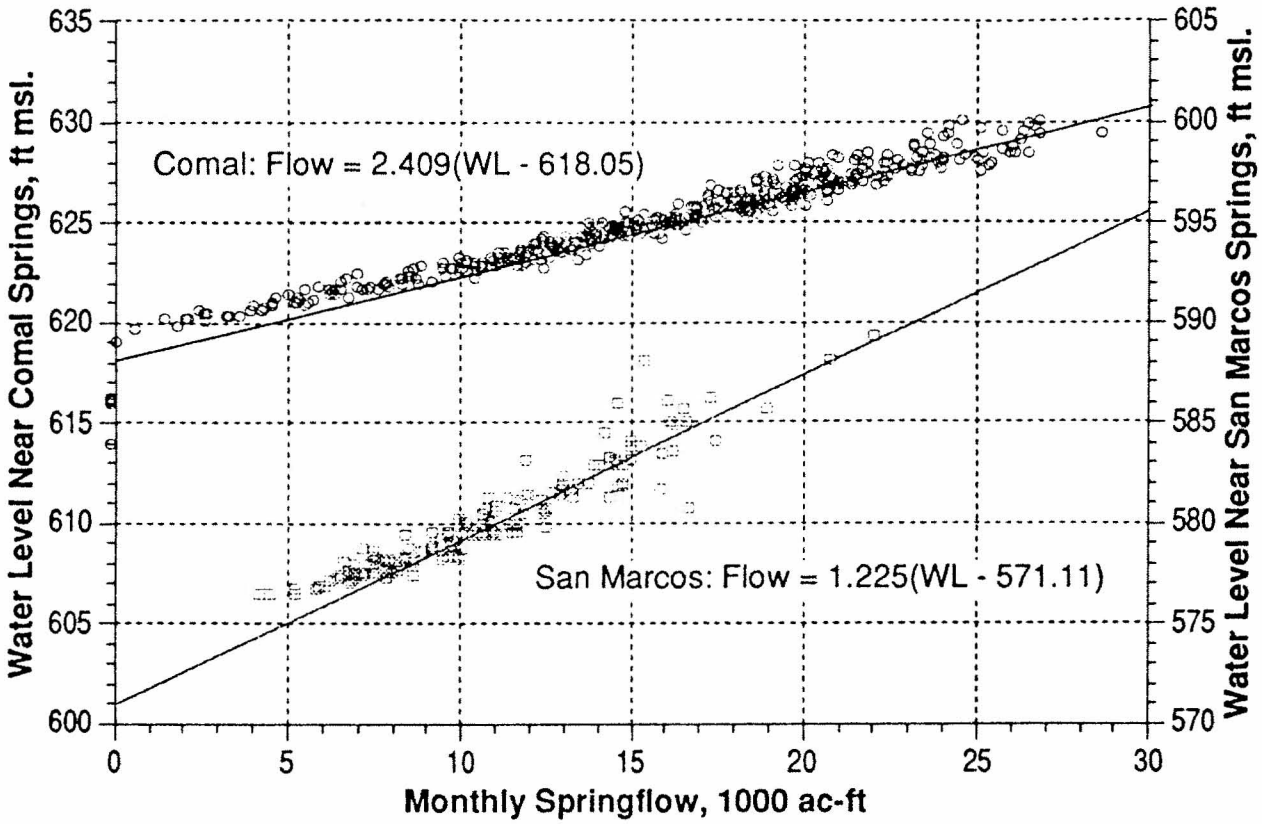

Figure 28. Relationship between springflows and water levels in the nearby wells

Minimizing $$f(x) = \sum_i (x_i - X_i)^2 \tag{38}$$

subject to $$g(x,u,T,S) = 0, \tag{39}$$

$$T_i \geq 0, \; S_i \geq 0, \text{ for all } i \tag{40}$$

where the objective function is the sum of squares of differences between observed and simulated water levels. Except variable bounds, the only constraint in this problem is the system of equations governing the simulation model. Solving this mathematical programming problem requires an interaction between an optimizer and the simulation. The optimizer used in this study is called GRG2 (Lasdon and Waren, 1986). The constraint subroutine is modified such that the simulation model is called to compute water levels before the objective function is evaluated. During each iteration, GRG2 assesses the current search status and suggests a new strategic set of parameters. The simulation model takes the parameters, and

computes a new set of water levels for GRG2. The iteration stops when an optimal set of parameters is obtained.

Typically, a few initial sets of guess parameter values must be used to avoid a local optimum. Due to the extreme nonlinearity in the nature of the simulation model, especially when the storage exponent is not at unity, steep valleys and ridges in constraint function are realized. Thus, a number of initial sets of parameters were attempted during the course of the calibration process. The best parameter values obtained by comparing all solutions are given in Appendix B as the model input. Results of the calibration are depicted in Figures 29-30.

Kalman Filtering

In this section we introduce a stochastic model and use it to condition the simulation results on the actual head measurements. Variability in input data and model simplification are common causes of uncetainty in the groundwater models. For this lumped parameter model, the input contains some variation due to errors in recharge and pumpage estimates and/or water level measurements although model assumptions are necessary to approximate reality. The model uncertainty can be extended from the deterministic model by introducing noise terms. If the statistics of system noise are known, an optimum filtering is usually used to quantify the model uncertainties. Kalman filtering is one of the widely used filtering techniques for hydrologic real time simulations. The rest of this section will explore how this filtering can improve the simulation results. The derivation of the algorithm can be found elsewhere (e.g. Sage and Melsa, 1976) and will not repeated. Consider the following system, a stochastic version of equation (6),

$$\mathbf{x}_{k+1} = \mathbf{P}_k\mathbf{x}_k + \mathbf{Q}_{u,k}\mathbf{u}_k + \mathbf{Q}_{w,k}\mathbf{w}_k \,, \tag{41}$$

$$\mathbf{y}_k = \mathbf{C}_k\mathbf{x}_k + \mathbf{v}_k \,, \tag{42}$$

where $\mathbf{u}_k$ is a deterministic input, $\mathbf{y}_k$ is the system measurable output, and $\mathbf{w}_k$ and $\mathbf{v}_k$ are the zero mean Gaussian noises for the system and output with the following covariance matrix:

$$E\left\{\begin{bmatrix}\mathbf{w}_k\\ \mathbf{v}_k\end{bmatrix}\begin{bmatrix}\mathbf{w}_k & \mathbf{v}_k\end{bmatrix}\right\} = \begin{bmatrix}\mathbf{W}_k & \mathbf{0}\\ \mathbf{0} & \mathbf{V}_k\end{bmatrix} \tag{43}$$

The Kalman filter algorithm is given as (Takahashi, et al., 1972):

$$\bar{\mathbf{x}}_{k+1} = \mathbf{P}_k\hat{\mathbf{x}}_k + \mathbf{Q}_{u,k}\mathbf{u}_k \tag{44}$$

$$\hat{\mathbf{x}}_{k+1} = \mathbf{K}_{k+1}\left\{\mathbf{y}_{k+1} - \mathbf{C}_{k+1}\bar{\mathbf{x}}_{k+1}\right\}, \qquad \hat{\mathbf{x}}_{-1} = \mathbf{0} \tag{45}$$

$$\mathbf{K}_{k+1} = \mathbf{M}_{k+1}\mathbf{C}_{k+1}^T\left(\mathbf{C}_{k+1}\mathbf{M}_{k+1}\mathbf{C}_{k+1}^T + \mathbf{V}_{k+1}\right)^{-1}, \tag{46}$$

$$\mathbf{M}_{k+1} = \mathbf{P}_k\mathbf{Z}_k\mathbf{P}_k^T + \mathbf{Q}_{w,k}\mathbf{W}_k\mathbf{Q}_{w,k}^T, \qquad \mathbf{M}_o = \left\{\mathbf{x}_o\mathbf{x}_o^T\right\} \tag{47}$$

$$\mathbf{Z}_k = (\mathbf{I} - \mathbf{K}_k\mathbf{C}_k)\mathbf{M}_k \tag{48}$$

where

$\bar{\mathbf{x}}_{k+1}$ is the simulated state vector (water levels) using the optimal linear estimate of the state vector;

$\hat{\mathbf{x}}_{k+1}$ is the updated state vector conditioned on the measured water levels;

$\mathbf{C}_k$ is the measurement matrix which transforms the simulated state vector to the output vector where measurements are available;

$\mathbf{M}_k$ is the covariance matrix of the simulated error, $\mathrm{Cov}(\mathbf{x}_k\text{-}\bar{\mathbf{x}}_k)$;

$\mathbf{Z}_k$ is the covariance matrix of the measurement update error, $\mathrm{Cov}(\mathbf{x}_k\text{-}\hat{\mathbf{x}}_k$;

$\mathbf{K}_k$ is the Kalman gain; and

$\mathbf{I}$ is the unity matrix.

In this study, the output matrix **C** is unity and we assume $\mathbf{Q}_{w,k} = \mathbf{Q}_{u,k}$. The covariances **W** and **V** are predetermined and fixed. The diagonal elements of **W** are determined from the variances of simulation errors while the measurement errors are assumed to have a standard error of 2 ft. The result of applying the Kalman filtering improved the simulation dramatically as shown in Figures 31 and 32.

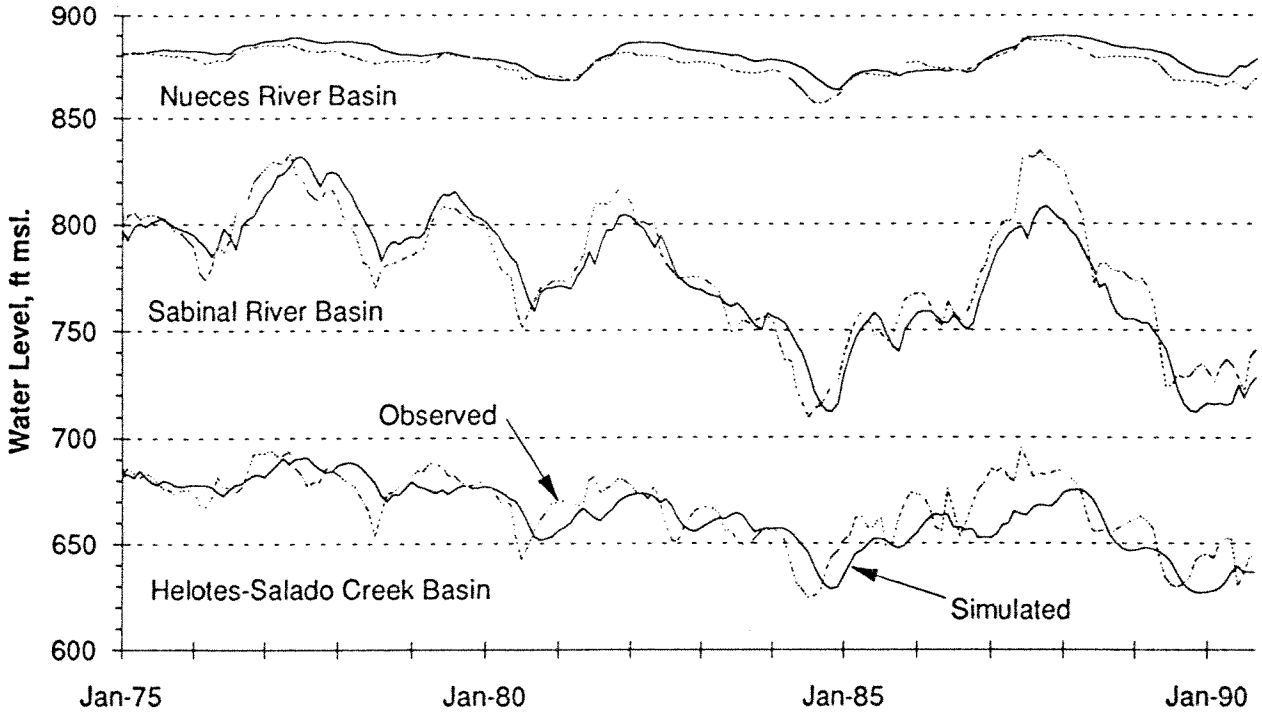

Figure 29. Comparision of the simulated and the observed water levels in selected river basins

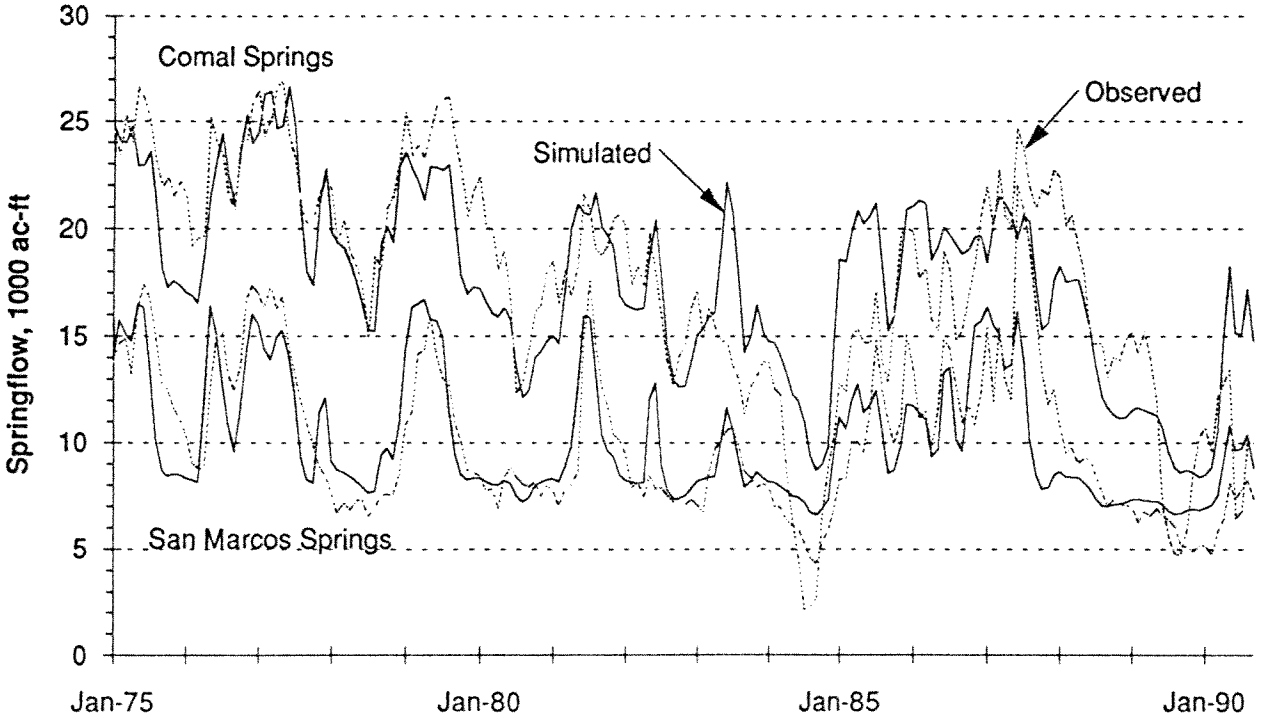

Figure 30. Comparision of the simulated and the observed springflows in the Comal and San Marcos Springs

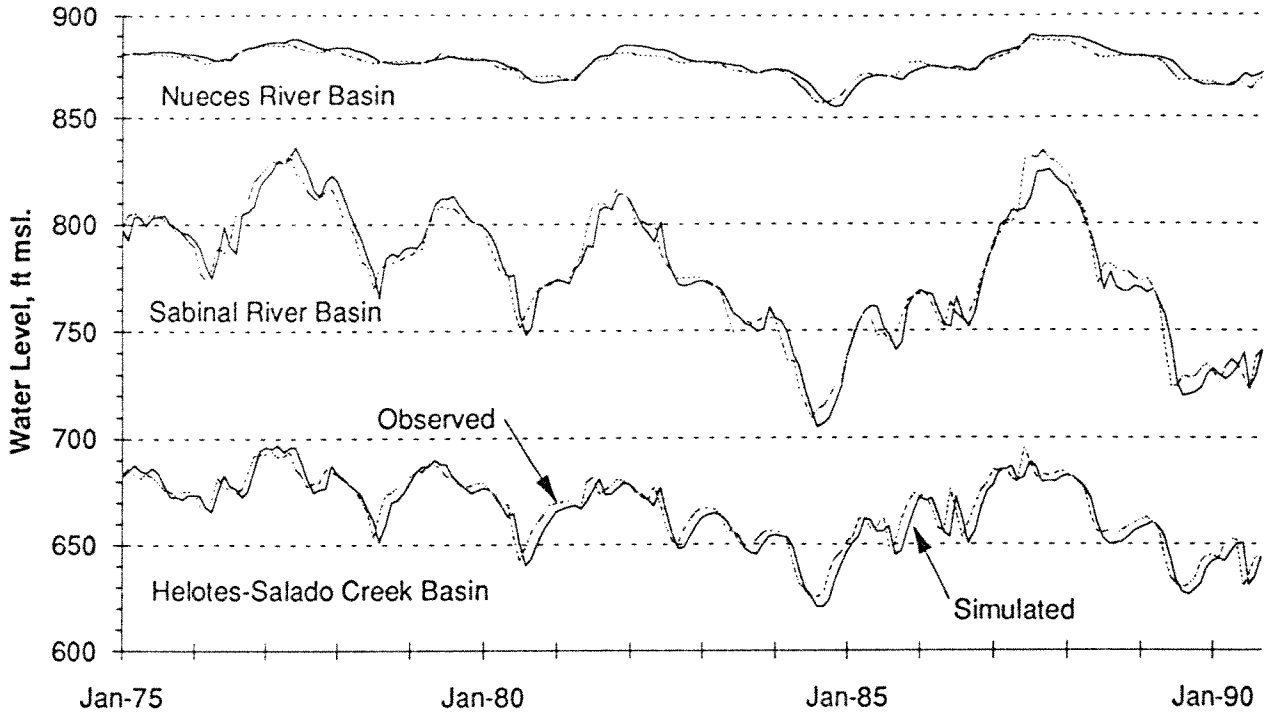

Figure 31. Comparision of the simulated and the observed water levels in selected river basins when applying the Kalman filter

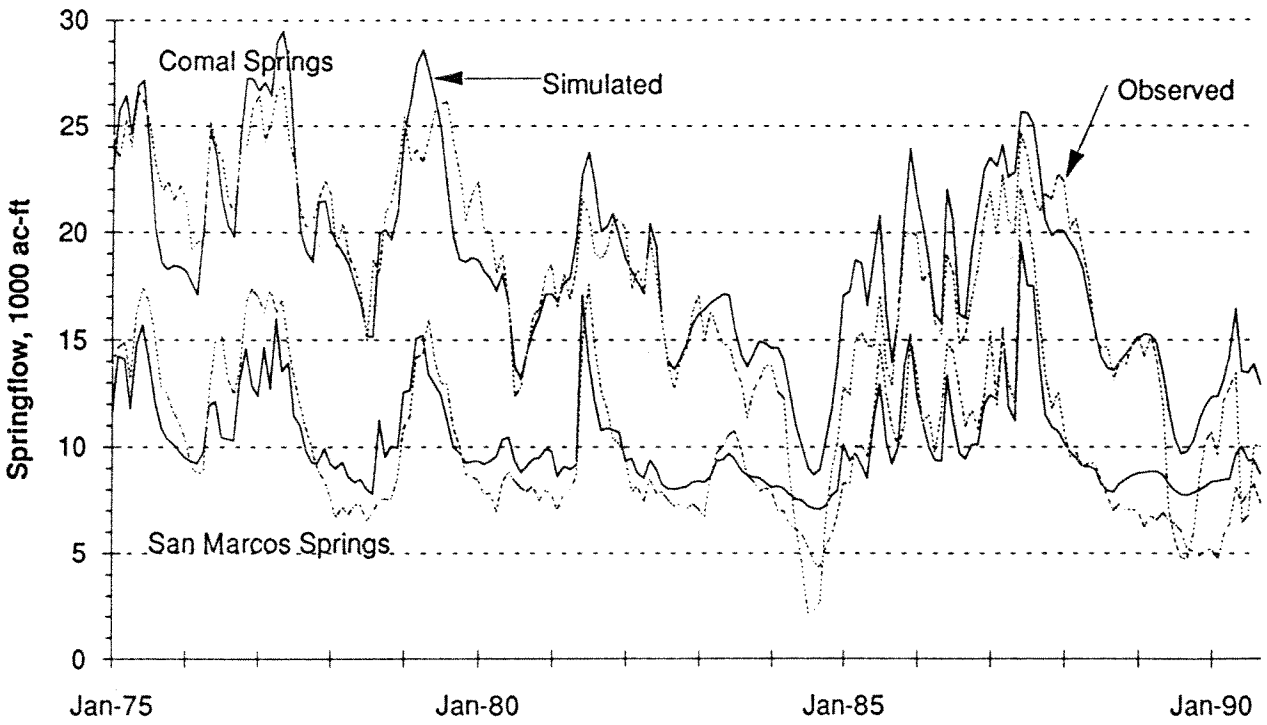

Figure 32. Comparision of the simulated and the observed springflows in the Comal and San Marcos Springs when applying the Kalman filter

Sensitivity Analysis

Sensitivity analysis was performed by comparing the results from small perturbations of system parameters. Only the storage and flow transmissivity related parameters were considered in this analysis. Figures 33-34 show changes of water levels as the transmissivity related parameters for all sub-basins are increased by 2, 5, and 10%. In effect, the groundwater flows faster from upstream basins to downstream basins and, thus, causes the water levels in the upstream basins to drop. However, when the parameter is increased in only a specific link, the hydraulic gradient in the link must drop to maintain the water balance in the system. As a result, the water levels will decrease in the upstream basin and increase in the downstream basin. These changes can be observed in Figures 35-38.

Sensitivity of the storage constant to the aquifer water levels is totally dependent on the basin. Generally, if storage related parameters are decreased, one should expect water levels to increase to maintain the same net flow in the water balance equation (Figures 39 and 40). This explanation is also applied to a small basins with a greater net inflow (Figures 43 and 44). Ironically, this is not the case for a larger basin with a small net flow, especially for the upstream basins (Figures 41 and 42).

In general, water levels are more sensitive to changes in storage related parameters than flow transmissivity related parameters. However, an increase in both parameters causes the water level to change in the opposite direction.

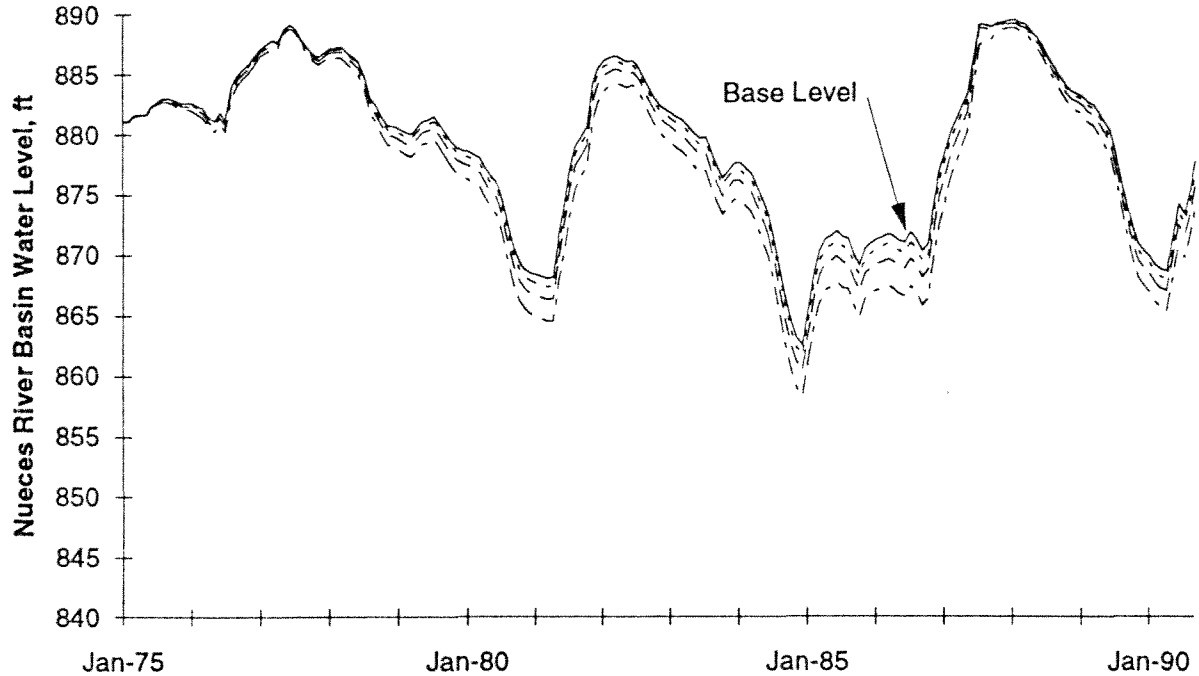

Figure 33. Water levels changes in the Nueces River Basin as all transmissivity related parameters are increased by 2, 5, and 10%

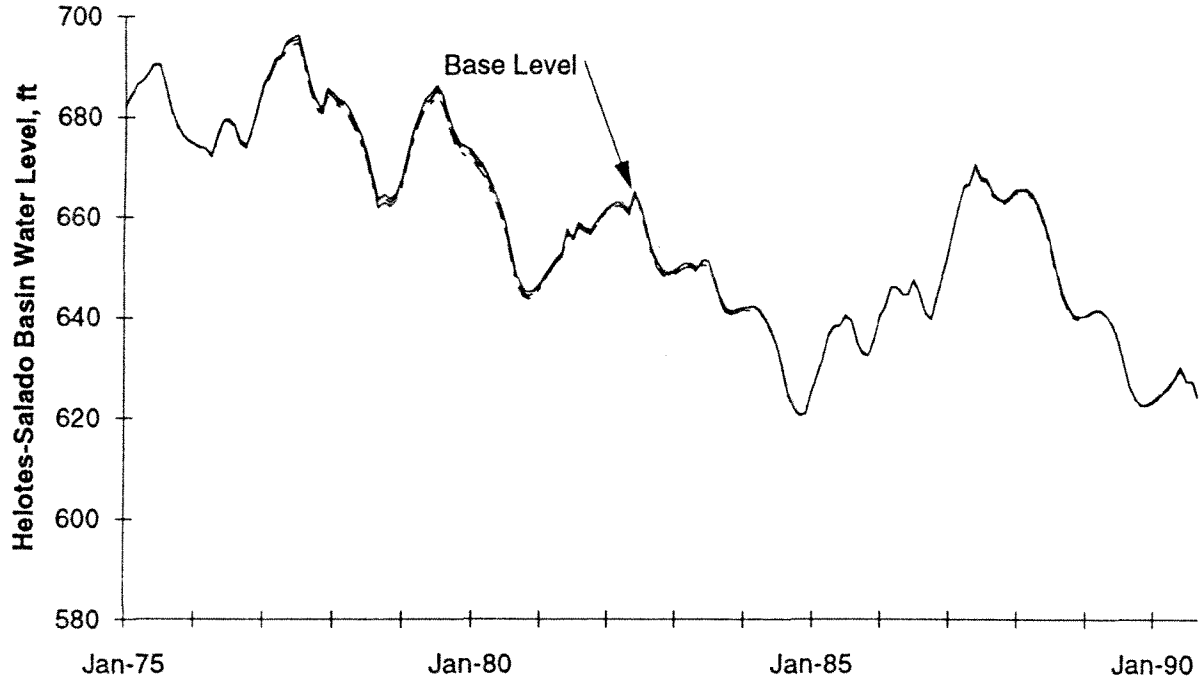

Figure 34. Water levels changes in the Helotes-Salado Creek Basin as all transmissivity related parameters are increased by 2, 5, and 10%

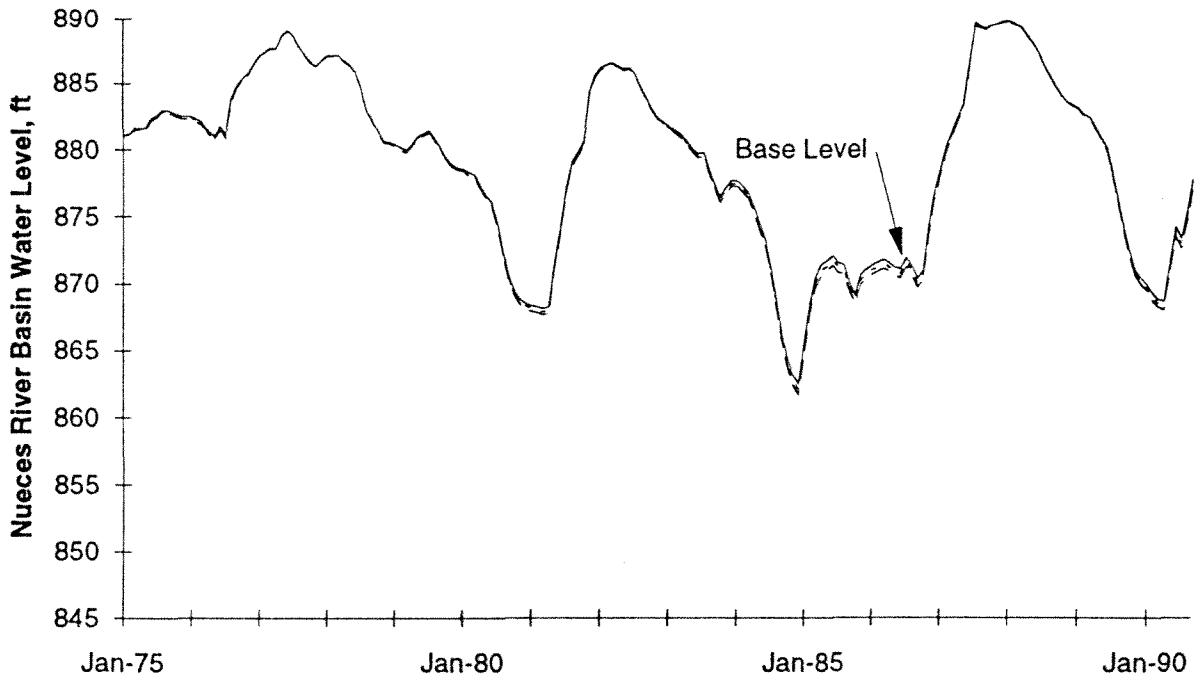

Figure 35. Water levels changes in the Nueces River Basin as the transmissivity related parameters in the link between Nueces and Frio River Basins are increased by 5 and 10%

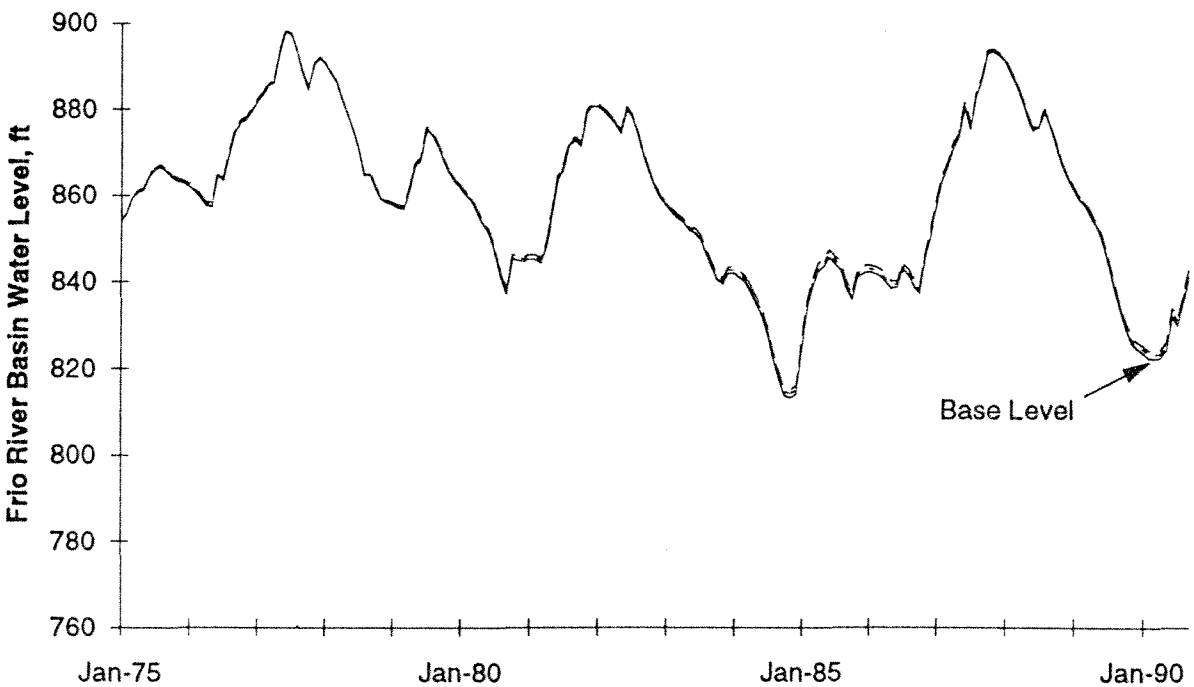

Figure 36. Water levels changes in the Frio River Basin as the transmissivity related parameters in the link between Nueces and Frio River Basins are increased by 5 and 10%

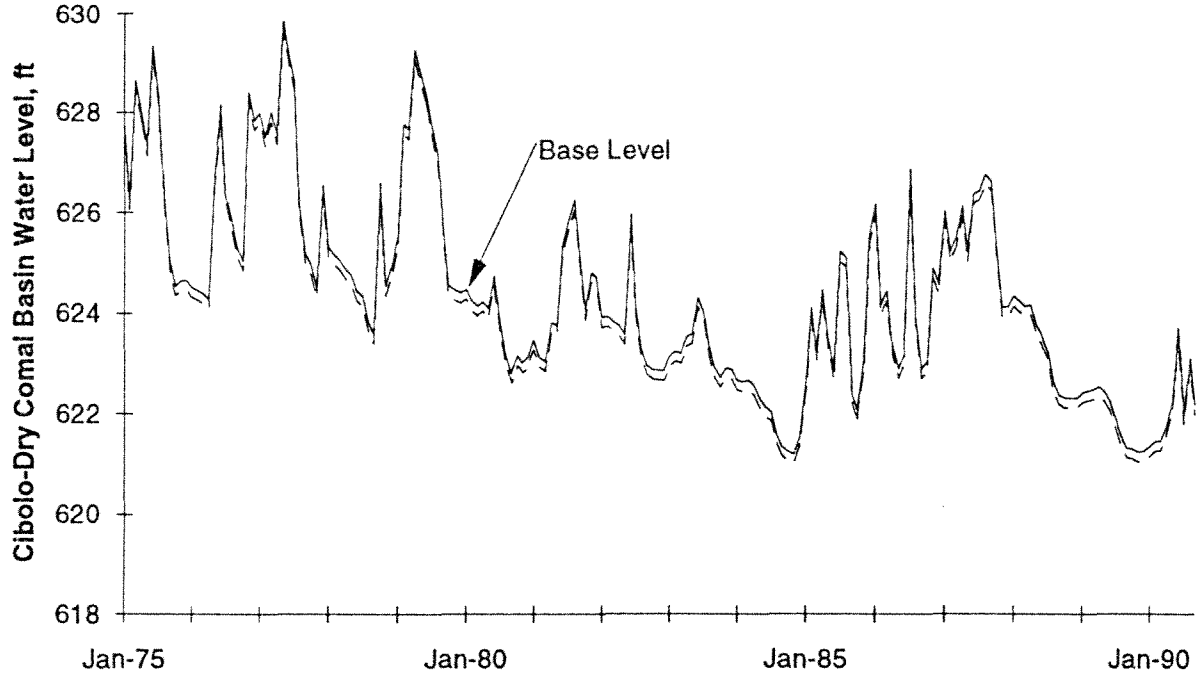

Figure 37. Water levels changes in the Cibolo-Dry Comal Creek Basin as the transmissivity related parameters in the link between Cibolo-Dry Comal and Blanco-Alligator River Basins are increased by 10%

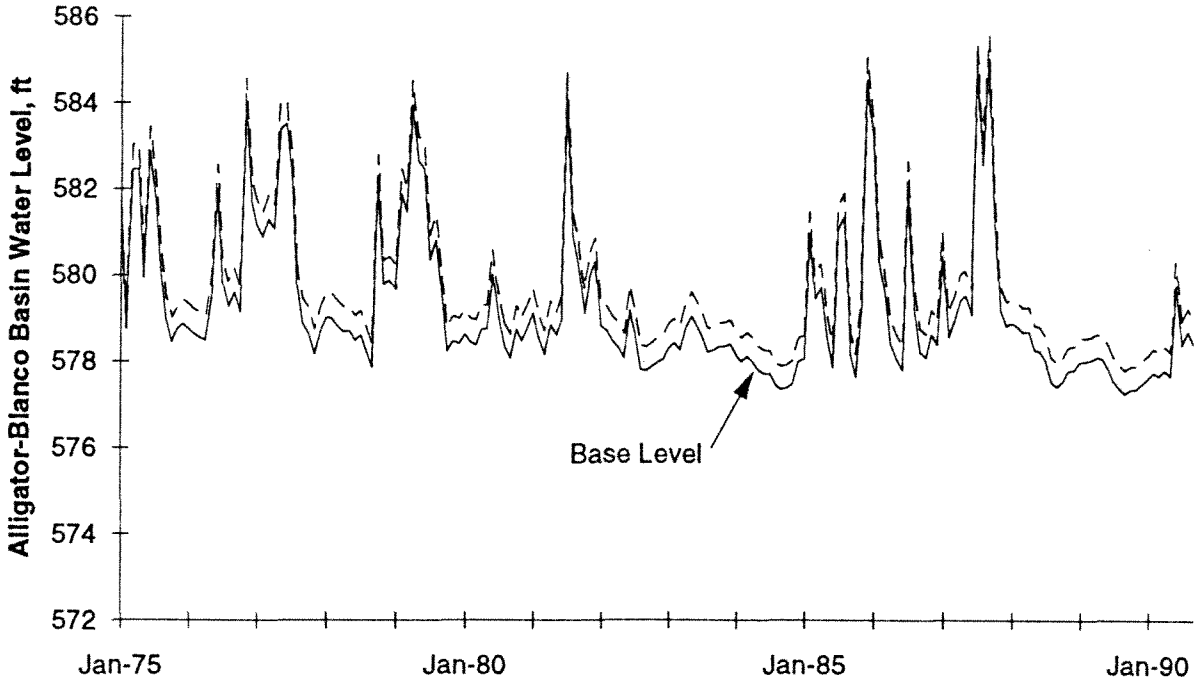

Figure 38. Water levels changes in the Alligator Creek-Blanco River Basin as the transmissivity related parameters in the link between Cibolo-Dry Comal Creek Basin and Alligator Creek-Blanco River Basin are increased by 10%

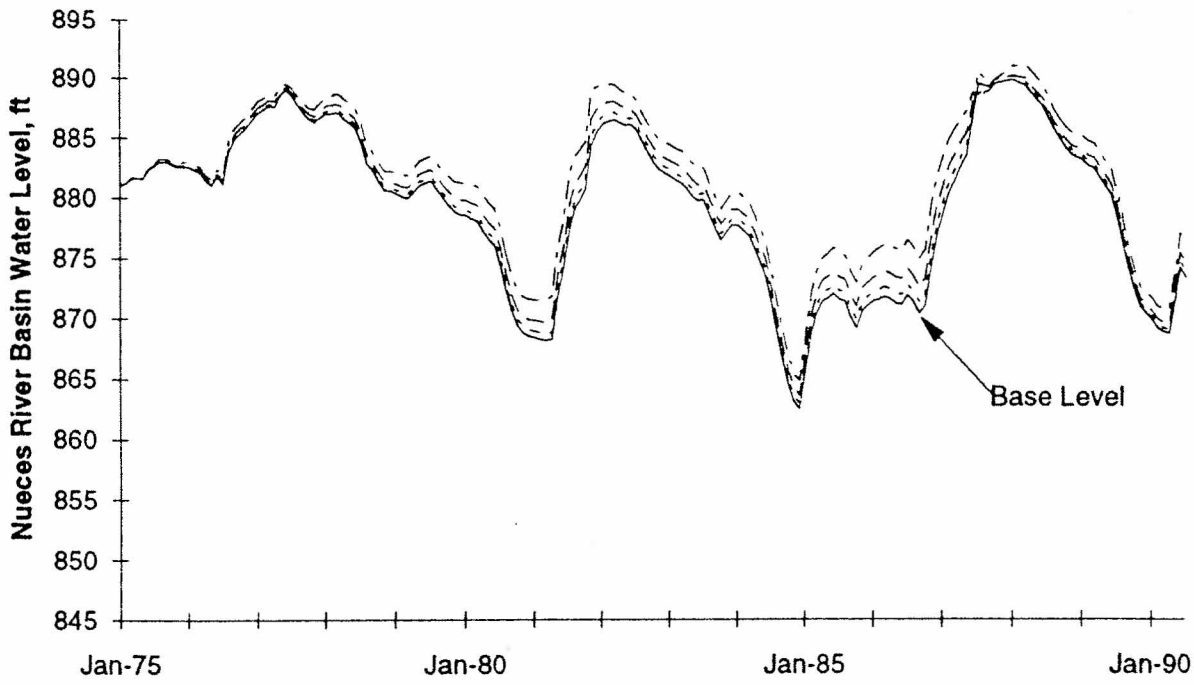

Figure 39. Water levels changes in the Nueces River Basin as all storage related parameters are decreased by 2, 5, and 10%

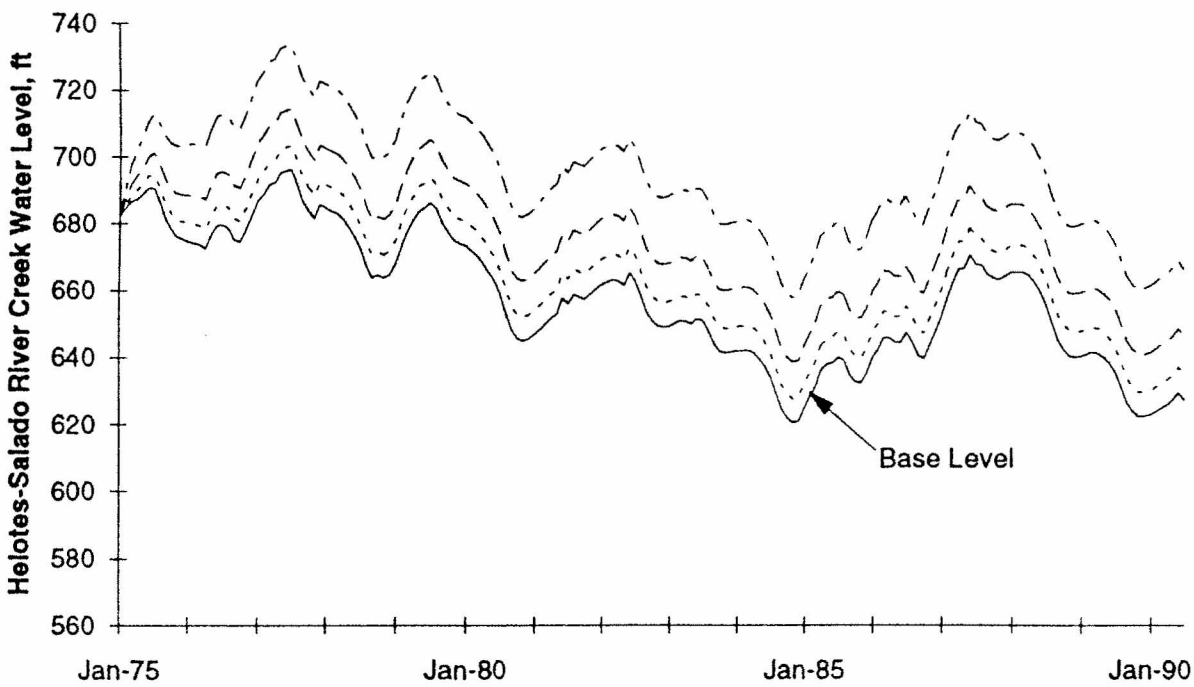

Figure 40. Water levels changes in the Helotes-Salado Creek Basin as all storage related parameters are decreased by 2, 5, and 10%

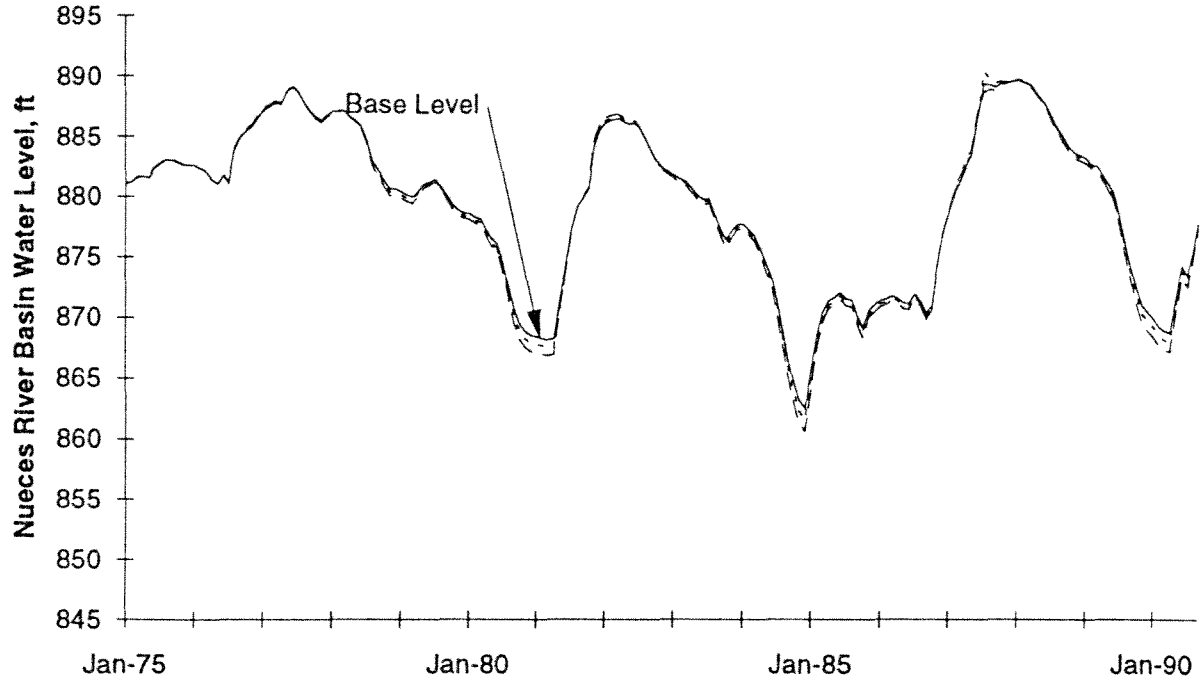

Figure 41. Water levels changes in the Nueces River Basin as its storage related parameters are decreased by 5 and 10%

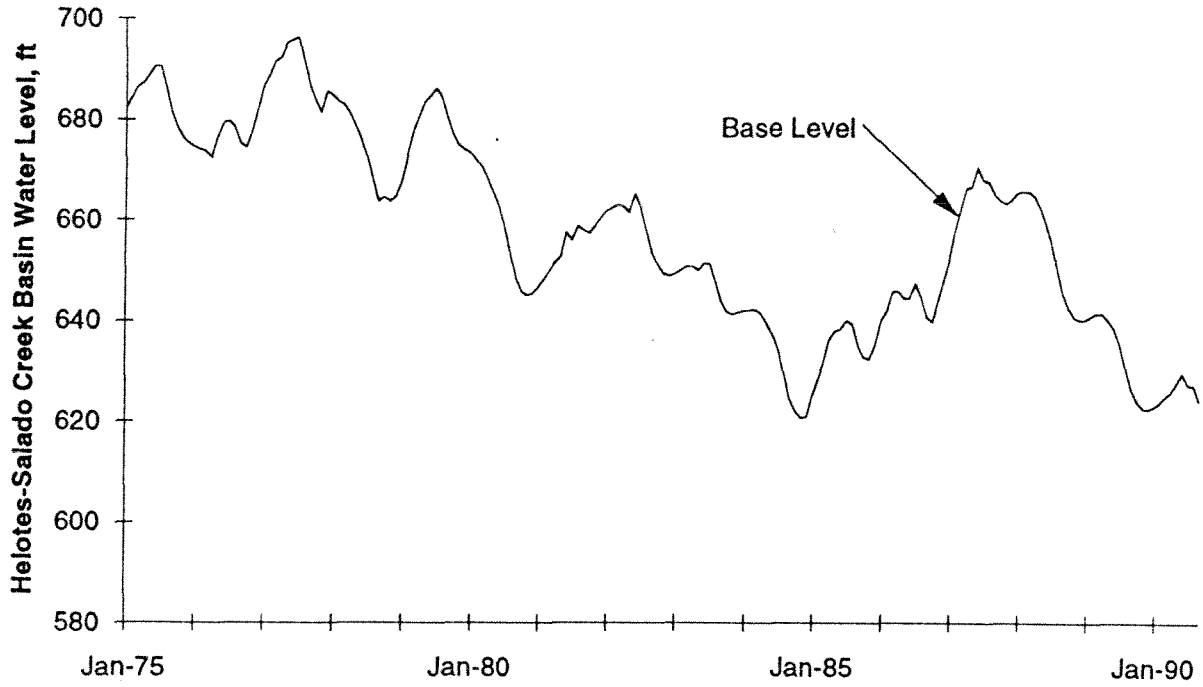

Figure 42. Water levels changes in the Helotes-Salado Creek Basin as the storage related parameters in the Nueces River Basin are decreased by 5 and 10%

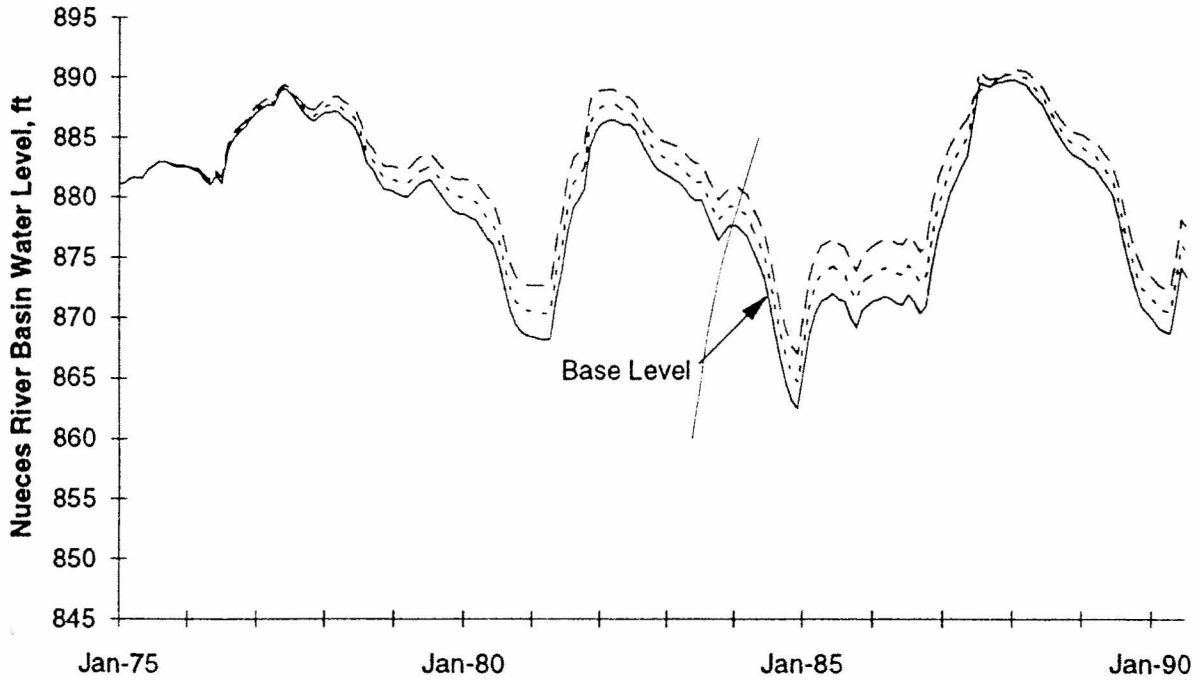

Figure 43. Water levels changes in the Nueces River Basin as the storage related parameters in the Helotes-Salado Creek Basin are decreased by 5 and 10%

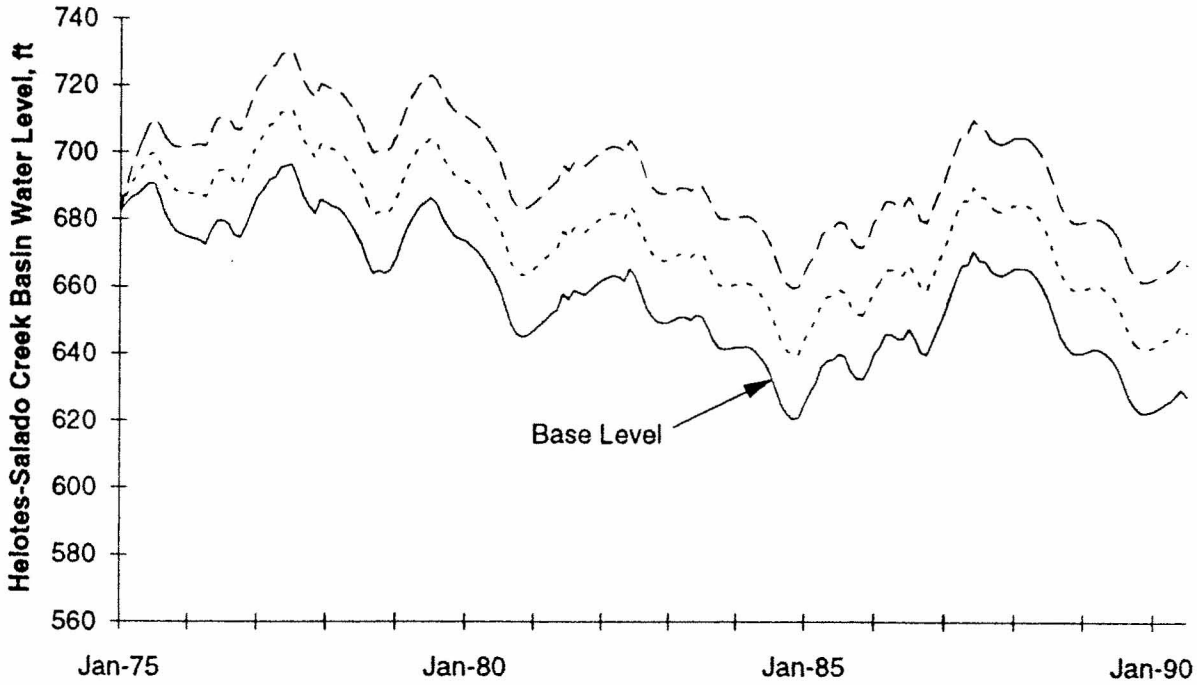

Figure 44. Water levels changes in the Helotes-Salado Creek Basin as its storage related parameters are decreased by 5 and 10%

SUMMARY AND CONCLUSIONS

A lumped parameter, conceptual tank-based model has been successfully applied and calibrated to the Edwards Aquifer. However, refinement and calibration should be done as soon as new data sets become available. The methodology has proved to be very efficient and provides good accuracy. Of 189 months, water levels in nine sub-basins and springflows at the Comal and San Marcos Springs were simulated in less than four minutes on an 68040 based microcomputer. The model is very easy to use since much less data is required, i.e., the average physical and hydrologic data for only nine basins is needed. We have planned to re-code the model as a spreadsheet function, which will allow the model to run inside a spreadsheet.

The success of model calibration suggests that the recharge functions incorporated in the model provide good estimates of monthly recharge. In addition, when summed to annual recharge estimates, the monthly recharge estimates from the recharge functions were very similar to recharge estimates by the USGS except for peak years. The method for estimating monthly recharge developed for the lump parameter model may be preferable to other methods for estimating recharge because the recharge functions **account for recharge capacity, water levels, and are less complex** than existing methods for estimating recharge.

Future research to improve model performance should include (1) the use of the Laplace transform as a solution method, (2) the generalization of the model for use with other karst aquifers, (3) exploration of ways to improve model accuracy such as; better recharge estimation, especially in the ungaged sub-basins of the Helotes, Salado and Dry Comal Creeks; re-delineating sub-basins to better represent regional flow patterns in the recharge zone; and implementing a non-linear regression for springflows and water levels, especially in the low flow regime.

Using the model for future research and study is suggested in different areas. First, the model can be easily integrated with a rainfall-runoff model so that the gage flows, which currently are inputs to the model, can be predicted from rainfall. Such an extension will be compatible with the use of rainfall to determine future pumpage management. Second, with the aid of a multi-site flow generator, reliabilities of aquifer management alternatives can be assessed. Using a stochastic model, water managers can explore the risk of various scenarios and make decisions without jeopardizing springflows below the regulated levels. Third, an aquifer

management model can be formulated using an optimization-simulation model. As a result, management alternatives can be evaluated and the best management plan can be selected. Finally, there will be a need for refining the model, perhaps to a daily operational model for use in the real-time pumpage regulation.

REFERENCES

Choffel, K. L. and S. K. Vaugh, 1993, Historical Recharge of the Edwards Aquifer in the Nueces, San Antonio, and Guadalupe River Basins. HDR Engineering, Inc. Proceedings: American Institute of Hydrology and American Water Resources Association Texas Sections Joint Meeting and Texas Hydrology Roundup, April 16,1993.

Garza, Sergio, 1966, Ground-Water Resources of the San Antonio Area, Texas, a progress report on studies, 1960-1964, Texas Water Development Board Report No. 34, Austin, Texas.

Klemt, W. B., T. R. Knowles, G. R. Elder, and T. W. Sieh, 1979, Ground-Water Resources and Model Applications for the Edwards (Balcones Fault Zone) Aquifer in the San Antonio Region, Texas. Texas Department of Water Resources Report, No. 239, Austin, Texas.

Lasdon, L. S., and A. D. Waren, 1986, "GRG2 User's Guide," School of Business Administration, University of Texas at Austin, Austin, Texas.

Lowry, R. L., 1955, Recharge to the Edwards Ground-Water Reservoir, Consulting Engineer Report to the San Antonio City Water Board, San Antonio, Texas.

Maclay, R. W. and L. F. Land, 1988, Simulation of Flow in the Edwards Aquifer, San Antonio Region, Texas, and Refinement of Storage and Flow Concepts. USGS Water- Supply Paper No. 2336-A, Denver, Colorado.

McDonald, M. G., and Harbaugh, A. W., 1988, A Modular Three-Dimensional Finite-Difference Ground-Water Flow Model, Techniques of Water Resources Investigations of the USGS, Book 6, Chapter A1, Denver, Colorado.

Prickett, T. A., and C. G. Lonnquist, 1971, Selected Digital Computer Techniques for Groundwater Resource Evaluation. Illinois State Water Survey Bulletin No. 55, Urbana, Illinois.

Puente, C, 1975, Relation of Precipitation to Annual Ground-Water Recharge in the Edwards Aquifer, San Antonio, Texas, USGS Open-File Report 75-298, Austin, Texas.

Puente, C, 1978, Method of Estimating Natural Recharge to the Edwards Aquifer in the San Antonio Area, Texas. USGS Water-Resources Investigations 78-10, Austin, Texas.

Sage, A. P., and J. L. Melsa, 1976, *Estimation Theory with Applications to Forecasting and Control*, McGraw-Hill, New York.

Takahashi, Y., M. J. Rabins, and D. M. Auslander, 1972, *Control and Dynamic Systems.* Addison-Wesley Publishing Co., Reading, Massachusetts, 2nd. edition.

Thorkildsen, D. and P. D. McElhaney, 1992, Model Refinement and Applications for the Edwards (Balcones Fault Zone) Aquifer in the San Antonio Region, Texas. Texas Water Development Board, Report No. 340, Austin, Texas.

Trescott, P. C., G. F. Pinder, and S. P. Larson, 1976, Finite-Difference Model for Aquifer Simulations in Two Dimensions with Results of Numerical Experiments. Techniques of Water-Resources Investigations of the USGS. Book 7, Chapter C1, Reston, Virginia.

van der Heijde, P. K. M., I. E. Aly, and S. A. Williams, 1988, "Groundwater Modeling: An Overview and Status Report," U. S. EPA 600/2-89/028, R. S. Kerr Environmental Research Laboratory, Ada, Oklahoma.

Wokhour, S., 1993, (Hydrogeologist: Edwards Underground Water District). Personal communication, August 1993.